

# Chemistry and Lithography

Vol. 2: Chemistry in Lithography

SECOND EDITION

Uzodinma Okoroanyanwu

**SPIE PRESS**

Bellingham, Washington USA

Library of Congress Cataloging-in-Publication Data

Names: Okoroanyanwu, Uzodinma, author. | Society of Photo-optical Instrumentation Engineers.

Title: Chemistry and lithography / Uzodinma Okoroanyanwu.

Description: Second edition. | Bellingham, Washington, USA : SPIE Press, 2020– | Includes bibliographical references and index. | Contents: volume. 2. Chemistry in lithography

Identifiers: LCCN 2019037747 | ISBN 9781510655577 (v. 2 ; hardback) | ISBN 9781510655584 (v. 2 ; pdf)

Subjects: LCSH: Lithography. | Chemistry, Technical. | Semiconductors–Etching.

Classification: LCC TP156.E68 O44 2020 | DDC 686.2/315–dc23

LC record available at <https://lccn.loc.gov/2019037747>

Published by

SPIE

P.O. Box 10

Bellingham, Washington 98227-0010 USA

Phone: +1 360.676.3290

Fax: +1 360.647.1445

Email: [books@spie.org](mailto:books@spie.org)

Web: <http://spie.org>

Copyright © 2023 Society of Photo-Optical Instrumentation Engineers (SPIE)

All rights reserved. No part of this publication may be reproduced or distributed in any form or by any means without written permission of the publisher.

The content of this book reflects the work and thought of the author. Every effort has been made to publish reliable and accurate information herein, but the publisher is not responsible for the validity of the information or for any outcomes resulting from reliance thereon.

Printed in the United States of America.

First printing.

For updates to this book, visit <http://spie.org> and type “PM353” in the search field.

**SPIE.**

# Contents

<i>General Preface to the Second Edition</i>	<i>xxiii</i>
<i>Acronyms and Abbreviations</i>	<i>xxix</i>
<b>PART I LITHOGRAPHIC PROCESS CHEMISTRY</b>	<b>1</b>
<b>1 Overview of Chemistry in Lithography</b>	<b>3</b>
<b>2 The Semiconductor Lithographic Process Chemistry</b>	<b>11</b>
2.1 Introduction	11
2.2 Wafer and Mask Priming Surface Chemistry	13
2.3 Resist Coating and Thin Film Instabilities	17
2.3.1 Resist spin-coating process	17
2.3.2 Characterizing ultrathin resist processes	22
2.3.3 Instabilities in UTR films	23
2.3.4 Spin coating and instabilities in UTR films	23
2.3.5 Hydrodynamics of UTR films	25
2.3.5.1 Instabilities and thermophysical properties of UTR films	27
2.3.6 Ultrathin film defectivity	32
2.3.6.1 Marangoni-effect-driven ultrathin film defects	33
2.3.6.1.1 Spin-coating defects and their origins	35
2.3.6.1.1.1 Chuck marks	35
2.3.6.1.1.2 Striations	37
2.3.6.1.1.3 Comets, streaks, or flares	37
2.3.6.1.1.4 Humidity-variation-caused defects	37
2.3.6.1.1.5 Wafer edge defects	38
2.3.6.1.2 The role of evaporation in spin-coating defects	39
2.3.6.1.2.1 Mechanism of capillary- driven flow instabilities in spin-coating systems	40
2.3.6.2 Non-Marangoni effect-driven ultrathin film defects	43
2.3.6.3 Patterning implications of UTR film instabilities	44

---

2.4	Resist Soft Bake Chemistry	45
2.5	Resist Exposure Chemistry	49
2.6	Resist Post-exposure Bake Chemistry	51
2.6.1	Deprotection kinetics of representative resist polymer systems	53
2.6.2	Monitoring PAG in thin photoresist films by means of fluorescence spectroscopy	58
2.6.3	PEB sensitivity	61
2.6.4	Consequences of acid diffusion	63
2.7	Resist Development Chemistry	64
2.7.1	Resist development methods	66
2.7.2	Types of development processes	67
2.7.2.1	Resist chemical development	67
2.7.2.2	Resist physical development	68
2.7.3	General mechanism of resist dissolution	69
2.7.3.1	Physical development mechanism	71
2.7.3.2	Chemical development mechanism	71
2.7.4	Solubility switching approaches to realizing contrast between exposed and unexposed regions of the resist during development	73
2.7.5	Development rate characterization	74
2.7.5.1	Laser interferometry	74
2.7.5.2	Quartz crystal microbalance	77
2.7.6	Dissolution mechanism of resist polymers	78
2.7.6.1	Dissolution mechanism of phenolic resists	79
2.7.6.1.1	Comparison of dissolution characteristics of novolac and PHOST-based resists	80
2.7.6.1.2	General facts about the dissolution mechanism of DNQ/novolac resists	81
2.7.6.1.3	Mechanistic models for DNQ/novolac dissolution	85
2.7.6.1.3.1	The membrane model	85
2.7.6.1.3.2	The secondary structure model	86
2.7.6.1.3.3	Critical deprotonation model	89
2.7.6.1.3.4	Percolation model of resist dissolution	92
2.7.6.1.3.5	Critical ionization model	94
2.7.6.1.3.6	Stone wall model of novolac dissolution	94

---

2.7.6.1.3.7	Effects of resin and inhibitor structure on dissolution rate	94
2.7.7	Resist development issues	98
2.7.7.1	Pattern collapse	98
2.8	Post-development Bake and Resist Stabilization Chemistry	104
2.8.1	Post-development bake	104
2.8.2	UV radiation curing	106
2.8.3	Electron beam curing of resists	108
2.8.3.1	Photochemical effects of electron beam curing of resists	110
2.8.3.2	Mechanical effects of electron beam curing of resists	111
2.9	Resist Etching Chemistry	112
2.9.1	Wet etching	112
2.9.2	Dry etching	114
2.9.2.1	Categories of dry chemical etching techniques	115
2.9.2.1.1	Plasma etching	115
2.9.2.1.2	Reactive ion etching	116
2.10	Resist Stripping Chemistry	117
<b>Part II LITHOGRAPHIC MATERIALS CHEMISTRY</b>		<b>119</b>
<b>3</b>	<b>Chemistry of the Lithographic Exposure Tool and Optical Element Materials</b>	<b>121</b>
3.1	Introduction	121
3.2	Chemistry of Lens Materials	121
3.2.1	Fused silica	125
3.2.2	Fused-silica degradation mechanisms	129
3.2.3	Calcium fluoride	131
3.2.4	Optical coatings	133
3.2.4.1	Aluminum mirrors	133
3.2.4.2	Dielectric optical coatings	134
3.2.5	Anti-reflection coatings	134
3.3	Chemistry of Mirror Materials	135
3.3.1	EUV multilayer mirrors	135
3.4	Chemistry of Lithographic Masks and Reticle Materials	135
3.4.1	X-ray masks	137
3.4.2	EUV masks	137
3.5	Lithographic Pellicles	138
3.5.1	Optical lithographic pellicles	138
3.5.2	EUV lithographic pellicles	140

---

<b>4</b>	<b>Chemistry of Lithographic Patterning Materials</b>	<b>141</b>
4.1	Introduction	141
4.2	Resists	141
4.2.1	Photoresist and radiation resist components	143
4.2.2	Nanoparticle resist components	144
4.2.3	Sol–gel resist components	144
4.2.4	Resist classification	144
4.2.5	Thermophysical, mechanical, and rheological properties of polymeric resist resins	148
4.2.5.1	Molecular weight properties of polymeric resist resins	150
4.2.5.2	Thermal properties of polymeric resist resins	150
4.2.5.3	Mechanical properties of polymeric resist resins	152
4.2.5.4	Viscoelastic properties of polymeric resist resins	154
4.2.5.5	Stress relaxation in polymeric resist resins	155
4.2.6	Resist solvents	155
4.2.7	Industrial manufacture of resist	157
4.3	Resist Developers and Rinses	158
4.4	Resist Strippers and Cleaners	161
4.5	Stone, Plate, and Offset Lithographic Inks	166
4.5.1	Stone and plate lithographic inks	166
4.5.2	Offset lithographic inks	166
4.5.3	Fountain solutions	166
<b>PART III LITHOGRAPHIC PHOTOCHEMISTRY AND RADIATION CHEMISTRY</b>		<b>167</b>
<b>5</b>	<b>Photochemistry and Radiation Chemistry in Lithography</b>	<b>169</b>
5.1	Introduction	169
5.2	General Considerations on Photochemistry, Photophysics, and Radiation Chemistry in Lithography	171
5.2.1	The phenomenon of light absorption in lithography	173
5.2.1.1	Absorbance, transmittance, molar absorption, and applications of the Beer–Lambert law in lithographic systems	176
5.2.1.2	Quantification of the strength or probability of absorption in lithographic systems	177
5.2.1.3	Effects of light absorption/excitation in lithographic systems	178
5.2.1.4	Deactivation of excited states	181
5.2.1.4.1	Competition between decay routes and quantum yield	182
5.2.1.5	Types of electronic transitions in lithographic systems	186

---

5.3	Radiation Chemistry versus Photochemistry in Lithography	186
5.4	Photochemistry of Optical Lithographic Exposure	
	Tool Sources	188
5.4.1	High-pressure arc lamps	188
5.4.2	Exciplex and excimer laser sources	190
5.4.2.1	Interaction between electromagnetic radiation exciplex and excimer lasing media: two-state systems and the Einstein coefficients	190
5.4.2.2	Lasing mechanism of rare-gas halide exciplex and diatomic halogen excimer lasers	193
5.4.2.3	Excitation schemes	196
5.4.2.4	Key operational parameters	197
5.4.3	EUV sources	199
5.4.3.1	Laser-produced plasma sources	201
5.4.3.2	Discharge-produced plasma sources	202
5.4.3.3	Free-electron laser sources	203
5.4.4	Electron sources	205
5.4.5	Ion sources	206
5.5	Photochemistry of Photon Interactions with Optical Elements, Masks, and Pellicles	206
5.5.1	Fused-silica degradation	207
5.5.2	Pellicle materials degradation	207
5.6	Photochemistry of Photon Interactions with the Exposure Medium	208
5.6.1	UV absorption properties of typical gases in lithographic exposure tools	210
5.6.2	Photodissociation of molecular oxygen	211
5.6.2.1	ArF laser photon-induced reactions of oxygen	214
5.7	Photochemistry of the Photo-oxidative Degradation of Photoresist Polymers	216
5.7.1	General mechanism of patterned resist polymer photo-oxidative degradation	217
5.7.2	Atomic oxygen reactions with polymers	219
5.7.3	Photo-oxygenation of polymers by singlet oxygen	220
5.8	Photochemistry of Mask and Exposure Tool Lens Contamination and Cleaning	221
5.8.1	Inorganic salt formation on DUV exposure tool lenses and reticles	221
5.8.1.1	Mechanism of ammonium sulfate crystal formation on DUV lithographic exposure lenses and reticles	222
5.8.1.1.1	Reaction pathways leading to the formation of ammonium sulfate crystals in DUV lithographic exposure tools	222

5.8.1.1.1	Direct oxidation of sulfur dioxide by stable atmospheric oxygen	223
5.8.1.1.2	Catalyzed oxidation of sulfur dioxide by metal ions	223
5.8.1.1.3	Photochemical oxidation of sulfur dioxide by ozone and hydroxyl radical	223
5.8.2	Photoinduced contamination of EUV optics and reticles	225
5.8.2.1	Carbon deposition	234
5.8.2.2	Oxidation	238
5.8.2.3	Impact of contamination	241
5.9	Contamination Mitigation Strategies in EUV Lithography	243
5.9.1	Exposure chamber environment control	244
5.9.2	Use of oxidation-resistant capping layers	244
5.9.3	Thermal processes used in EUV optics contamination mitigation	244
5.9.4	Nonthermal processes used in EUV optics contamination mitigation	246
5.9.5	Reactive ion etching processes for cleaning contaminated optics	250
5.9.6	Debris mitigation schemes	250
5.10	Photochemistry and Radiation Chemistry of Defect Repair of Optical Lithographic Masks	250
5.10.1	Photochemistry of laser repair of lithographic mask defects	250
5.10.2	Radiation chemistry of focused-ion-beam repair of lithographic mask defects	251
5.10.3	Radiation chemistry of focused electron beam repair of lithographic mask defects	251
5.11	Photochemistry and Radiation Chemistry of Resist Systems	252
5.11.1	Photochemistry of resist exposure	252
5.11.1.1	Electronically excited-state complexes in resist systems	254
5.11.1.1.1	Excimers	254
5.11.1.1.2	Exciplexes	257
5.11.1.2	Bimolecular interactions, quenching, and energy transfer in lithographic systems	257
5.11.1.2.1	Quenching processes of excited states in lithographic systems	257
5.11.1.2.1.1	Energy transfer in quenching processes in lithography	258
5.11.1.3	Energy migration in resist polymers	267
5.11.1.4	Spectral sensitization	270



---

5.11.1.4.1	Spectral sensitization modes	272
5.11.1.4.1.1	Triplet sensitization	272
5.11.1.4.1.2	Sensitization by electron transfer	274
5.11.2	Aspects of the radiation chemistry of resists	276
5.11.3	Resist sensitivity to electromagnetic radiation	277
5.11.4	Resist exposure mechanisms	278
5.11.5	Radiation chemistry of resist polymers	283
5.11.5.1	Radiation chemical yield and dosimetry	284
5.11.5.2	Backbone scission and crosslinking	284
5.11.5.3	Determination of the scission yield	285
5.11.5.4	Determination of the crosslinking yield $G_x$	287
5.11.6	Photochemistry of photoactive compounds	287
5.11.6.1	Photochemistry of photoacid generators	288
5.11.6.1.1	Ionic PAGs	288
5.11.6.1.1.1	Aryldiazonium salts	289
5.11.6.1.1.2	Diaryliodonium salts	290
5.11.6.1.1.3	Triarylsulfonium salts	293
5.11.6.1.2	Nonionic photoacid generators	296
5.11.6.1.2.1	Nitrobenzyl esters	297
5.11.6.1.2.2	Sulfones	299
5.11.6.1.2.3	Phosphates	302
5.11.6.1.2.4	Arylsulfonate esters	302
5.11.6.1.2.5	Iminosulfonate and imidosulfonate esters	303
5.11.6.1.2.6	Diazonaphthoquinones	306
5.11.6.1.2.7	Natural product-based PAGs	311
5.11.6.2	Photochemistry of photobase generators	311
5.11.6.2.1	O-acyloximes	311
5.11.6.2.2	Benzyloxycarbonyl and o-nitrobenzyloxycarbonyl derivatives	313
5.11.6.3	Photochemistry of photodecomposable bases	313
5.11.6.4	Photochemistry of photosensitizers	317
<b>PART IV CHEMISTRY OF LITHOGRAPHIC IMAGING MECHANISMS</b>		<b>319</b>
<b>6</b>	<b>Chemistry of Photochemical and Radiochemical Imaging Mechanisms of Negative-Tone Resists</b>	<b>321</b>
6.1	Introduction	321
6.2	Resins	322
6.3	Types of Negative Resists	323
6.3.1	Non-radiation-based negative resists	323
6.3.1.1	Wax–lampblack–soap resists	323
6.3.2	Radiation-induced negative resists	324

---

6.3.2.1	Negative resists based on radiation-induced crosslinking reactions	324
6.3.2.1.1	Negative resists based on crosslink formation by direct reactions of excited chromophores	325
6.3.2.1.1.1	Bitumen resists	325
6.3.2.1.1.2	Cinnamate resists	326
6.3.2.1.1.3	Poly(vinyl cinnamylidene acetate) resists	329
6.3.2.1.1.4	Chalcone and polyester resists	330
6.3.2.1.1.5	Polyimide resists	331
6.3.2.1.1.6	Water-processable negative resists incorporating ionizable groups	332
6.3.2.1.2	Negative resists based on crosslink formation by radiation-generated reactive species	333
6.3.2.1.2.1	Non-chemically amplified crosslinking negative resists	333
6.3.2.1.2.2	Negative resists based on crosslinking by radicals	349
6.3.2.2	Negative resists based on radiation-induced polarity changes	363
6.3.2.2.1	Non-chemically amplified negative resists based on radiation-induced polarity changes	364
6.3.2.2.1.1	Metal-chalcogenide resists	364
6.3.2.2.1.2	Imaging mechanisms of $\text{Ag}_2\text{Se}/\text{Ge-Se}$ resists	368
6.3.2.2.1.3	Ylide resists	370
6.3.2.2.1.4	Diazo resists	370
6.3.2.3	Chemically amplified negative resists based on radiation-induced polarity changes	372
6.3.2.3.1	Chemically amplified negative resists based on an acid-catalyzed pinacol rearrangement	372
6.3.2.3.2	Chemically amplified negative resists based on acid-catalyzed intramolecular dehydration	374

---

6.3.2.3.3	Chemically amplified, condensation/ intermolecular dehydration negative resists based on acid-catalyzed crosslinking with acid-sensitive electrophile (crosslinking agent)	376
6.3.2.3.4	Chemically amplified methacrylate negative resists based on acid-catalyzed esterification	384
6.3.2.3.5	Chemically amplified methacrylate negative resists based on acid-catalyzed deprotection and development in supercritical CO <sub>2</sub>	387
6.3.2.3.6	Negative resists based on ligand exchange reactions	390
6.4	General Considerations on the Chemistry of Crosslinking	392
6.5	Negative Resists Based on the Polymerization of Monomers in the Presence of Polyfunctional Components	395
6.5.1	Composition of negative resists based on photopolymerization	396
6.5.2	Binders	397
6.6	General Considerations on the Chemistry of Photoinitiated Radical Polymerization Employed in Negative Resist Systems	397
6.6.1	Photogeneration of radicals	398
6.6.1.1	Initiators based on photofragmentation	399
6.6.1.1.1	Peroxides	399
6.6.1.1.2	Azo compounds	399
6.6.1.1.2.1	Benzoin derivatives	400
6.6.1.1.2.2	Acetophenone derivatives	401
6.6.1.1.2.3	Ketoxime esters of benzoin	402
6.6.1.1.2.4	Triazines	403
6.6.2	Radicals generated by hydrogen abstraction	403
6.6.2.1	Benzophenone and tertiary amines	404
6.6.2.2	Michler's ketone	405
6.6.2.3	Thioxanthenes	406
6.6.2.4	3-Ketocoumarins	406
6.6.3	Dye-sensitized initiation	406
6.6.4	The initiation step	410
6.6.5	Propagation versus termination and the kinetic chain length	411
6.6.5.1	The steady state approximation	411
6.7	General Considerations on Photoinitiated Condensation Polymerization	413
6.7.1	The thiol-ene system	413
6.8	General Considerations on the Photoinitiated Cationic Polymerization Employed in Negative Resist Systems	414

---

6.8.1	Onium salt-initiated cationic polymerization	414
6.8.1.1	Initiation	415
6.8.1.2	Propagation	415
6.8.2	Epoxy-based negative resists based on a cationic crosslinking reaction mechanism	418
6.8.2.1	SU-8 resist	418
6.8.2.2	Fullerene/epoxy resists	419
6.8.2.3	Multi-trigger negative-tone epoxy-based molecular resists	422
6.8.2.4	Polystyrene/allyl glycidyl epoxy negative resists	425
6.8.3	Limitations of negative-tone resists based on cationic polymerization-induced crosslinking	426
6.9	Vapor-Deposited, Dry-Developed Metal Salts, Organometallic, and Metalorganic Oxide Hard Mask Resists	428
6.10	Lithographic Applications of Photopolymerization Negative Resists	429
6.10.1	Lithographic offset plates	430
6.10.2	Dry resists	431
6.10.3	Printed circuit boards	431
6.10.4	Solder masks	432
6.10.5	IC device fabrication	432
<b>7</b>	<b>Chemistry of Photochemical and Radiochemical Imaging Mechanisms of Positive-Tone Resists</b>	<b>435</b>
7.1	Introduction	435
7.2	Types of Positive Resists	437
7.2.1	Non-chemically amplified positive resists	437
7.2.1.1	Non-chemically amplified positive resists based on functional group polarity switch	437
7.2.1.1.1	Dissolution-inhibition resists	437
7.2.1.1.1.1	Diazonaphthoquinone/novolac resists	437
7.2.1.1.1.2	Diazo-Meldrum's acid-based resists	468
7.2.1.1.1.3	Resists based on ortho-nitrobenzyl chemistry	469
7.2.1.1.1.4	Resists based on photo-Friess rearrangement	473
7.2.1.2	Non-chemically amplified positive resists based on main-chain scission	475
7.2.1.2.1	Resists based on poly(methyl methacrylate) and its derivatives	475
7.2.1.2.1.1	Poly(methyl isopropenyl ketone) resists	484
7.2.1.2.1.2	Poly(olefin sulfone) resists	485

---

7.2.1.2.1.3	Poly(chloroacrylate-co- $\alpha$ -methylstyrene) resists	488
7.2.2	Chemically amplified positive resists: the chemical amplification concept	489
7.2.2.1	Acid generators	490
7.2.2.2	Chemically amplified positive resists and their imaging mechanisms	498
7.2.2.2.1	Chemically amplified positive resists based on a functional group polarity switch	499
7.2.2.2.1.1	Chemically amplified positive resists based on deprotection	499
7.2.2.2.1.2	Chemically amplified positive resists based on Claisen rearrangement	542
7.2.2.2.1.3	Chemically amplified positive resists based on depolymerization	544
7.3	Resist Materials for Multilayer Resist Systems	549
7.3.1	Hard mask resist material	550
7.3.2	Top surface imaging resists	551
7.3.3	Bilayer resists	551
<b>8</b>	<b>Chemistry of the Limiting Issues of Photochemical and Radiochemical Resists and Approaches to Their Solutions</b>	<b>555</b>
8.1	Introduction	555
8.2	Chemical Aspects of Advanced Resist Processing Techniques	559
8.2.1	Single-exposure techniques	560
8.2.1.1	Hyper-NA imaging resist processing techniques	560
8.2.1.2	EUV lithography resist processing technique	560
8.2.2	Post-exposure-based CD shrink techniques	561
8.2.2.1	Reflow CD shrink techniques	562
8.2.2.1.1	Thermal reflow shrink technique	562
8.2.2.1.2	Electron-beam-induced CD shrink techniques	562
8.2.2.2	Chemically induced CD shrink techniques	564
8.2.2.2.1	Chemically induced CD shrink techniques based on sidewall formation	564
8.2.2.2.1.1	Resolution enhancement of lithography assisted by chemical shrink (RELACS™)	565

	8.2.2.2.1.2	Chemical amplification of resist lines (CARL) process scheme	566
	8.2.2.2.2	Chemically induced CD shrink techniques based on sidewall erosion	566
	8.2.2.2.2.1	Hydrophilic overlayer (HOL) process	567
	8.2.2.2.3	Plasma-assisted CD shrink technique	570
8.3		Resolution Limit Issues of Resists	571
	8.3.1	Resolution limits due to chemical amplification in resists	571
	8.3.1.1	Elucidating how photoacid diffusion leads to resist contrast and resolution loss	578
	8.3.1.2	Resolution limits due to line edge roughness	579
	8.3.1.3	Base quenchers	581
	8.3.1.4	Polymer size	581
	8.3.1.5	Shot noise	582
	8.3.2	Resolution limits due to confinement effects in resists	584
	8.3.3	Resolution limits due to resist polymer molecular properties	586
	8.3.4	Resolution–LER–sensitivity trade-off challenges	586
	8.3.5	Complex CAR behavior in EUV lithography	589
	8.3.5.1	Stochastic effects	589
	8.3.5.2	Pitch-dependent blur effects	591
	8.3.5.3	Sensitivity to out-of-band radiation	592
	8.3.6	Approaches to overcoming the chemical amplification drawbacks in resists	594
	8.3.6.1	Polymer-bound photoacid generators	595
	8.3.6.2	Photodecomposable bases	596
	8.3.6.3	Multi-trigger resist concept	597
	8.3.6.4	Photosensitized CAR concept	600
	8.3.6.4.1	Mechanism of version 1 PSCAR materials	601
	8.3.6.4.2	Mechanism of version 2 PSCAR materials	603
8.4		Vapor Deposited, Dry Developed Metal Salts, Organometallic, and Metalorganic Oxide Hard Mask Resists	604
8.5		Resist Materials Outlook for the Advanced Technology Nodes	606
8.6		Resist Processing Outlook for the Advanced Technology Nodes	607
<b>9</b>		<b>Chemistry of Self-Assembling Lithographic Imaging Mechanisms</b>	<b>609</b>
	9.1	Introduction	609
	9.2	Block Copolymer Self-Assembly	611
	9.2.1	Block copolymer synthesis	617

---

9.2.1.1	Block copolymers via anionic polymerization	622
9.2.1.1.1	General mechanism of anionic polymerization	624
9.2.1.1.1.1	Initiation	625
9.2.1.1.1.2	Propagation	627
9.2.1.1.1.3	Termination	627
9.2.1.1.2	Kinetics of anionic polymerization	628
9.2.1.1.3	General experimental procedures	632
9.2.1.1.3.1	Synthesis of AB diblock copolymers	633
9.2.1.1.3.2	Synthesis of linear triblock copolymers	641
9.2.2	Block copolymer synthesis via controlled radical polymerization	648
9.2.2.1	Block copolymers synthesis via atom transfer polymerization (ATRP)	648
9.2.2.2	Block copolymer synthesis via stable free-radical polymerization (SFRP)	649
9.2.2.2.1	Synthesis of block copolymers containing styrene and styrenic derivative blocks	651
9.2.2.2.2	Synthesis of block copolymers containing dienes with styrene, acrylate, or methacrylate derivative blocks	653
9.2.3	Block copolymers synthesis via cationic polymerization	654
9.2.3.1	General mechanism of cationic polymerization	656
9.2.3.1.1	Initiation	656
9.2.3.1.2	Propagation	656
9.2.3.1.3	Chain transfer	657
9.2.3.1.4	Termination	657
9.2.3.2	Synthesis of representative diblock copolymers by cationic polymerization	657
9.2.3.2.1	Synthesis of block copolymers containing styrene and isobutylene blocks	658
9.2.3.2.2	Synthesis of block copolymers containing vinyl ethers and styrenic blocks	660
9.2.4	Improving chemical and thermal stability of block copolymers	660
9.2.5	Physics of micro- and nanophase separation in block copolymer systems	662
9.2.5.1	Phase formation and construction in a symmetric AB diblock copolymer melt	666

---

9.2.5.2	AB diblock copolymer configurations	670
9.2.6	Domain orientational control and long-range ordering	672
9.2.6.1	Neutral brushes for perpendicular alignment	673
9.2.6.2	Lithographically directed block copolymer directed self-assembly	676
9.2.6.2.1	Chemoepitaxy DSA lithography	676
9.2.6.2.2	Graphoepitaxy DSA lithography	681
9.2.6.3	Solvent annealing	683
9.2.6.4	Other methods used for aligning the orientation of self-assembling block copolymers	684
9.2.6.4.1	Application of external fields	684
9.2.6.4.2	Contact line pinning	686
9.2.6.4.3	Directional crystallization	686
9.2.6.4.4	Shear alignment	687
9.2.6.4.5	Soft lithography	688
9.2.7	Scaling block copolymer domain periodicity	688
9.2.8	Outlook for directed block copolymer self-assembly lithography	692
9.3	Colloidal Particle Self-Assembly Lithography	693
9.4	Monomolecular-Layer Self-Assembly Lithography	696
9.5	Outlook for Directed Self-Assembly Lithography	698
<b>10</b>	<b>Chemistry of Imprint Lithographic Imaging Mechanisms</b>	<b>701</b>
10.1	Introduction	701
10.2	Imprint Techniques	702
10.2.1	Thermal imprint lithography	702
10.2.2	UV imprint lithography	702
10.2.3	Solvent-assisted imprint lithography	703
10.2.4	Electrochemical imprint lithography	705
10.3	Imprint Tools and Materials	706
10.3.1	Imprint resist materials	706
10.3.1.1	Polymeric imprint resist materials	707
10.3.1.2	Nanoparticle imprint resist materials	710
10.3.1.3	Sol-gel imprint resist materials	710
10.3.2	Imprint stamp materials	714
10.3.3	Imprint stamp release materials	715
10.4	Imprint Lithographic Imaging Mechanisms	716
10.4.1	Thermal imprint lithographic imaging mechanism	716
10.4.2	UV imprint lithographic imaging mechanism	718
10.4.3	Peculiar issues of UV-IL and T-IL	719
10.5	Theoretical Models of the Imprinting Process	719
10.5.1	General considerations on the viscoelastic properties of polymers	719
10.5.2	Squeezing flow theory of the imprint process	722



---

<b>PART V LITHOGRAPHIC-PROCESS-INDUCED CHEMISTRY</b>	<b>729</b>
<b>11 Lithographic Electrochemistry</b>	<b>731</b>
11.1 Introduction	731
11.1.1 Corrosion in lithography	731
11.1.1.1 Corrosion types	732
11.1.1.2 Electrostatic discharge	733
11.1.2 Electrochemical imprint lithography	737
11.2 Corrosion/Oxidation of Chrome Structures in DUV Lithographic Masks	738
11.2.1 Mechanism of lithographic mask chrome structure oxidation	739
11.2.1.1 Crevice corrosion of lithographic masks	739
11.2.1.2 Pitting corrosion of lithographic masks	740
11.2.1.3 Kinetics of pitting and crevice corrosion of lithographic masks	741
11.3 Mechanism of Electrochemical Imprint Lithography	743
<b>12 Lithographic Colloidal Chemistry</b>	<b>747</b>
12.1 Introduction	747
12.2 The Forces Involved in Lithographic Colloidal Stability	750
12.2.1 Charged lithographic colloids	751
12.2.1.1 Formation of charged colloids in aqueous lithographic colloidal solutions	751
12.2.1.2 General electrostatic interaction forces operating in lithographic colloidal solution	752
12.2.1.3 Theory of the diffuse electrical double layer	753
12.2.1.4 The Debye length	757
12.2.1.5 Surface charge density	758
12.2.1.6 Zeta potential of a colloidal particle	760
12.2.1.7 The Hückel equation ( $\kappa a < 0.1$ )	760
12.2.1.8 The Smoluchowski equation ( $\kappa a > 100$ )	762
12.2.1.9 Interaction between double layers	766
12.2.1.10 The Derjaguin approximation	769
12.2.2 The DLVO theory of colloidal stability	770
<i>Index</i>	<b>773</b>

# Chapter 1

## Overview of Chemistry in Lithography

“I do not feel obliged to believe that the same God who has endowed us with sense, reason, and intellect has intended us to forgo their use.”

Galileo Galilei, Letter to the Grand Duchess Christina

In this volume we explore the chemical basis of pattern formation in advanced lithography, which in all its essential aspects is about chemical transformations that are designed to print a relief image of an object on a flat surface or a surface with topography. The object may be a mask containing patterns of integrated circuit devices; the flat surface may be a silicon wafer coated with photo- or radiation-sensitive resist, which upon exposure and development, or imprinting (as in the case of imprint resists) or directed self-assembly [(DSA) as in the case of block copolymer resists], is transformed into the relief image of the mask. Underlying some of these transformations are distinct chemical reactions that are mediated by electrons. By drawing on fundamental, theoretical, and experimental studies of molecular processes in advanced lithography, we deconstruct lithography into its essential chemical principles and situate its various aspects in specific fields of chemistry. We examine and show how electrons mediate the photo- and radiation chemistry of exposure processes of resists (be they organic, organometallic, polymeric, or inorganic), as well as exposure tool sources (be they mercury arc lamp, laser, electron beam, ion beam, or plasma); colloid chemistry of resist formulation and dissolution (be it for positive-tone or negative-tone development), wafer and mask cleaning processes; electrochemistry of mask absorber corrosion, electrostatic discharge, and electromigration; surface chemistry of wafer and mask priming, along with thin film interfacial effects; materials chemistry of resists, exposure tool optics, and masks; environmental chemistry of the exposure environment (be it water, air, or vacuum) as well as of resist poisoning; process chemistry and modeling of wafer and mask-making lithographic unit operations, including substrate priming, coating, exposure,

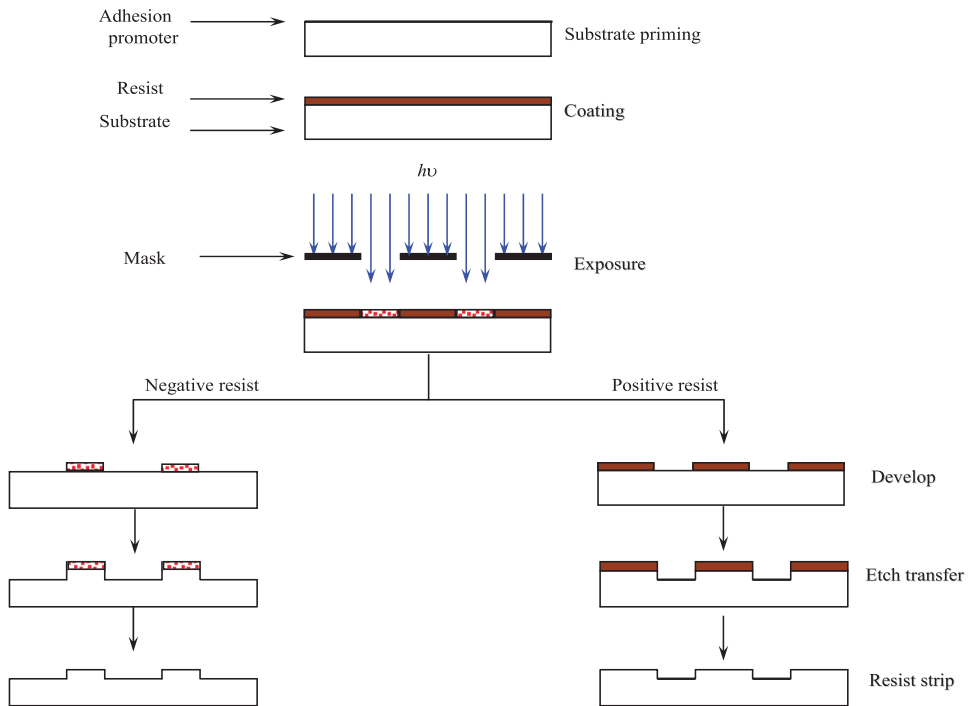


**Figure 1.2** The semiconductor lithographic process, showing the unit operations involved.

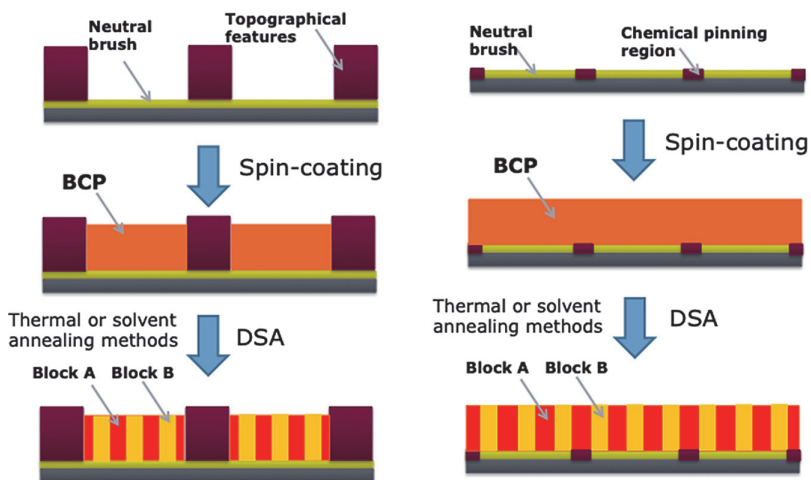


**Figure 1.3** Block copolymer self-assembly lithographic processes: (left) graphoepitaxy and (right) chemoepitaxy.

# Chapter 2

## The Semiconductor Lithographic Process Chemistry

“That’s how it is,” says Pooh.  
A.A. Milne, *Now We Are Six*

### 2.1 Introduction

Within a semiconductor fabrication facility, popularly called a “fab,” the lithography module occupies a very central position, literally in terms of the device fabrication process flow as well as in terms of the importance of the role it plays. Lithography is often considered the most critical step in integrated circuit (IC) fabrication, for it defines the critical dimension—the most difficult dimension to control during fabrication (e.g., polysilicon gate length)—of the device. This explains why the critical dimension (CD) in lithography is often used to define the device technology node or generation.<sup>1</sup> It is estimated that lithography accounts for nearly one-third of the total wafer fabrication cost.<sup>2</sup>

The object of semiconductor lithography is to transfer patterns of ICs drawn on the mask or reticle to the semiconductor wafer substrate. The transfer is carried out by projecting the image of the reticle with the aid of appropriate optical elements of an exposure tool onto a radiation-sensitive resist material coated on the semiconductor wafer, typically made of silicon, and stepping the imaging field across the entire wafer to complete a layer. The shape of the IC pattern transferred to the wafer substrate is entirely dependent

---

<sup>1</sup>M. Quirk and J. Serda, *Semiconductor Manufacturing Technology*, Prentice-Hall, New Jersey, pp. 336–337 (2001).

<sup>2</sup>S. Campbell, *The Science and Engineering of Microelectronic Fabrication*, Oxford University Press, New York, p. 152 (1996).

## 2.3 Resist Coating and Thin Film Instabilities

After priming, the wafer is coated with a liquid solution of BARC (in the case of spin-on BARCs), baked, and cooled, before it is coated with a liquid solution of resist. Wafers with inorganic CVD BARCs are coated with resists immediately after priming. There are several methods of coating resists on wafers: spin coating, spray coating, and dip coating. The most widely used methods for coating resist in the semiconductor industry are spin-coating methods.

### 2.3.1 Resist spin-coating process

In the spin-coating process, a precise amount of liquid resist is dispensed onto a wafer (either statically, i.e., with the wafer at rest, or dynamically, i.e., with the wafer rotating). The wafer is then spun at high speeds until the film thickness reaches a desired value, oftentimes corresponding to a stationary point on the swing curve of the given resist (Fig. 2.4). The process thus uses the dynamics of centrifugal forces to disperse a fluid of polymeric resist material over the entire wafer surface. The flow and rheological properties of the resist do influence the coating process and need to be considered to achieve optimal results.<sup>16</sup> The final thickness and properties of the spin-coated film depend on the nature of the resist solution (viscosity, evaporation rate, percent solids, surface tension) and spin-coating parameters such as final rotation speed, acceleration, and fume exhaust.

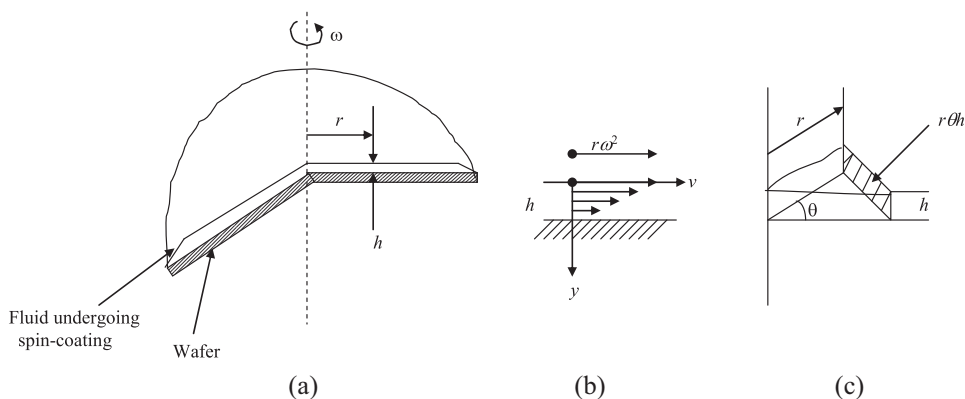


**Figure 2.4** Schematics of the spin-coating process, showing (a) liquid flow on a rotating wafer, (b) the velocity profile of the flowing liquid, and (c) a cross-section of a wedge-shaped portion of the flowing liquid.

<sup>16</sup>D. E. Bornside, C. W. Macosko, and L. E. Scriven, "Modeling of spin coating," *J. Imag. Tech.* **13**, pp. 122–130 (1987).

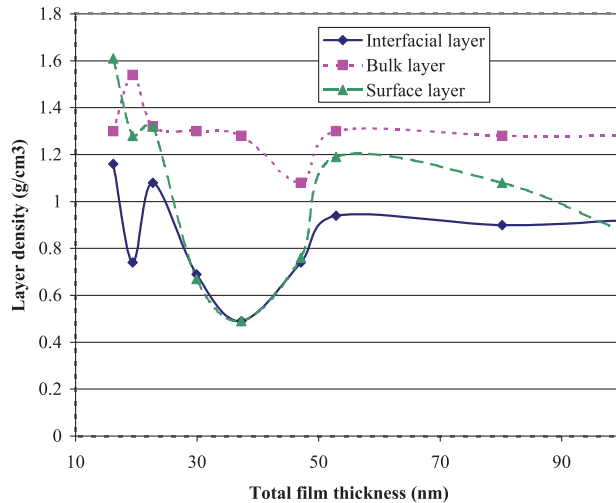


**Figure 2.9** Film layer density as a function of total film thickness as determined by x-ray reflectivity. The resist used was Shipley XP-98248 resist. (Reprinted from Okoroanyanwu.<sup>63</sup>)

monomeric units of the polymer in this region of the film. These also suggest the onset of thin film instabilities in this thickness range.<sup>64</sup>

Figure 2.10 shows a plot of film layer roughness as a function of total film thickness of XP-98248 resist as determined by fitting the XRR data. While the surface layer is relatively smooth [roughness measured by XRR was  $\sim 0.4\text{--}0.5$  nm, compared to the  $\sim 0.2\text{--}0.3$ -nm RMS value obtained with the atomic force microscope (AFM)] through the total film thickness range of 16–100 nm, that of the interface between the bulk and surface layer shows significant fluctuations between  $\sim 0.4$  and 2.7 nm within this thickness range. The film–substrate interface layer, on the other hand, is smooth (roughness  $\sim 0.5$  nm) in the 47- to 100-nm total film thickness range, below which it shows significant roughness of up to 4.0 nm at a thickness of 30 nm. This result indicates the influence of film–substrate interfacial effects and consequently thin film instabilities.<sup>65</sup>

### 2.3.6 Ultrathin film defectivity

UTR film defects fall into two main categories based on the mechanism of their origin: Marangoni-effect-driven defects and non-Marangoni effect-driven defects. Both defect types are discussed below.

<sup>63</sup>ibid.

<sup>64</sup>ibid.

<sup>65</sup>ibid.

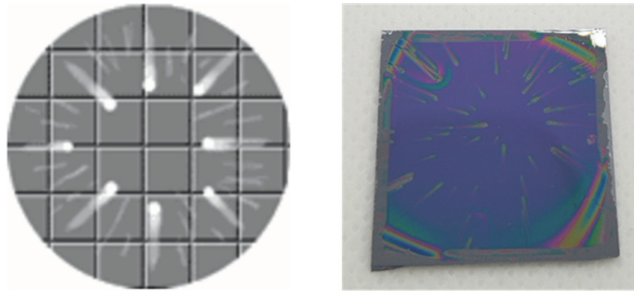


**Figure 2.13** Images of comets obtained on a film spin-coated onto a silicon wafer: (left)<sup>93</sup> and (right).<sup>94</sup>

The effects can manifest as roughness, microcracking of the coating upon further drying, etc.

#### 2.3.6.1.1.5 Wafer edge defects

The centrifugal force that underpins the spin-coating process is not uniform throughout the entire wafer; rather, it scales linearly with the radius, with the wafer edge experiencing the highest magnitude of the force. Complicating this process is the fact that once the radially outward flowing solution reaches the edge of the wafer, surface tension effects can make it difficult for the solution to detach from the wafer. A “bead” of liquid can stay attached around the entire perimeter of the wafer, resulting in thicker coatings in this rim zone than at inner locations on the wafer (Fig. 2.14). This results in coating nonuniformity. For substrates that are not round (for example, square or rectangular substrates), the air flow over their corners during spin coating are

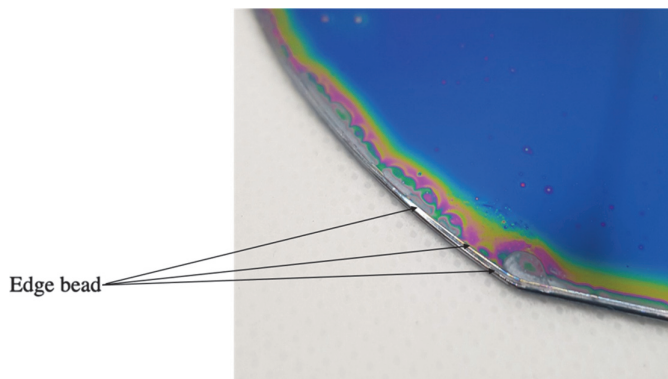


**Figure 2.14** Optical image of edge bead defects on a silicon wafer.<sup>95</sup>

<sup>93</sup><https://www.brewerscience.com/processing-theories/spin-coat/>

<sup>94</sup>Image from Daeon Jung, University of Massachusetts Amherst.

<sup>95</sup>ibid.

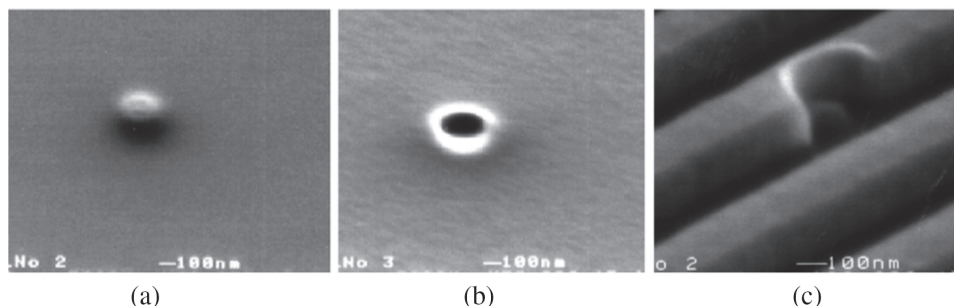


**Figure 2.18** Evolution of a bubble defect (a) formed at the resist coating, (b) through development, and (c) patterning with the ASML PAS5500/300 KrF stepper. Unexposed resist loss for the UTR film was  $\sim 6$ – $10$  nm. The poly-Si patterns are 180-nm lines and spaces. Film thickness was  $\sim 100$  nm. (Reprinted from Okoroanyanwu.<sup>112</sup>)

### 2.3.6.3 Patterning implications of UTR film instabilities

Given the enhanced surface mobility, which is a consequence of the decreased surface density—hence, the increased free volume of UTR film surfaces relative to the bulk and that of the film/substrate interfacial region—the lithographic properties of UTR films are bound to be dominated by interfacial effects. The surface region of such films is usually saturated with water or other solvents that can act as plasticizers. Thus, the  $T_g$  value of the surface chains can be further lowered with respect to the bulk chains.<sup>113</sup> The differences between the surface and bulk properties of UTR films can have a significant influence on their dissolution, etching, and diffusional properties.<sup>114</sup>

Figure 2.19 shows SEM images of line-and-space patterns printed with  $\sim 60$ -nm-thick XP-98248 resist on bare silicon and exposed at 157 nm, highlighting the dominant influence of polymer cooperative and surface dynamics near the surface region and interfacial effects related to polymer packing constraints near the substrate region. Poor profiles such as these are also obtained when the same film is processed on anti-reflection coatings (ARCs), implying that the poor lithographic performance of this UTR film cannot be solely due to the reflective swing effects from the silicon substrate. Significant undercutting suggests enhanced dissolution in the film–substrate interfacial region relative to the bulk layer. This is consistent with the XRR results obtained on a similar film of the same resist (see Fig. 2.9), which show the film–substrate interface layer to have a lower density than the bulk layer. This may also be related to polymer chain packing constraints and weak

<sup>112</sup>ibid.

<sup>113</sup>F. Garbassi, M. Morra, and E. Ochiello, *Polymer Surfaces: From Physics to Technology*, 2<sup>nd</sup> edition, John Wiley & Sons, New York (1998).

<sup>114</sup>U. Okoroanyanwu, “Thin film instabilities and implications for ultra-thin resist processes,” *J. Vac. Sci. Technol. B* **18**(6), 3381–3387 (2000); U. Okoroanyanwu, “Limits of ultra-thin resist processes,” *Future Fab International* **10**, 157–163 (2001).



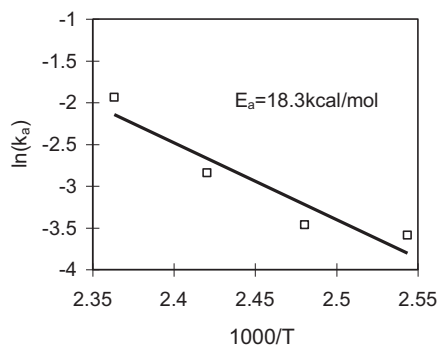


**Figure 2.28** Arrhenius plot for resist formulated with poly(CBN-*co*-MAH) and exposed under 193-nm radiation. (Reprinted from Okoroanyanwu Byers, Cao, et al.<sup>153</sup>)

sulfonium hexafluoroantimonate (TPSHFA) PAG. The activation energy for the deprotection of the pendant-*t*-butyl group of resists formulated with poly(CBN-*co*-NBCA) made by Pd(II)-catalyzed addition and free radical polymerization techniques was determined to be 6.7 and 9.4 kcal/mol, respectively, over the temperature range of 120 to 150 °C. Figure 2.28 is an Arrhenius-type plot of the deprotection kinetics of resist formulated with poly(CBN-*co*-MAH). The activation energy for the deprotection of the pendant-*t*-butyl group of resist polymer was determined to be 18.3 kcal/mol over the temperature range of 120 to 150 °C. This Arrhenius relationship is not considered valid outside of the region experimentally covered.

The thermal decomposition of DNQs in novolac resist film follows pseudo-first-order reaction kinetics (see Fig. 2.29). The 2,1,4-DNQ photoactive compound (PAC) is more thermally stable than the 2,1,5-DNQs, the activation energy difference between the two isomers being 8 kcal/mole.<sup>154</sup>

### 2.6.2 Monitoring PAG in thin photoresist films by means of fluorescence spectroscopy

Fluorescence spectroscopic techniques are being used increasingly in a wide range of research fields including biochemical, medical, and chemical research, primarily because of their inherent sensitivity and the favorable time scale of the phenomenon of fluorescence.<sup>155</sup> Some fluorophores have dramatically different emission characteristics in their protonated and unprotonated forms. Using this phenomenon, the photoacid concentrations generated within chemically amplified photoresist systems can be

<sup>153</sup>ibid.

<sup>154</sup>W. M. Moreau, "Thermal stability of naphthodiazquinone sensitizers," *Proc. SPIE* **3049**, 618–627 (1997).

<sup>155</sup>J. R. Lackowicz, *Principles of Fluorescence Spectroscopy*, Plenum Press, New York, Chapters 1 & 2 (1986).

Exposure-induced chain scissioning that leads to reduction of resist polymer molecular weight is another approach to effecting polarity switching, and hence improving contrast between the exposed and unexposed regions of the film during solvent development. From Flory–Huggins theory discussed in Chapter 3, it can be appreciated that the enthalpic term must be essentially the same in both the starting polymer and the scissioned polymer, indicating that dissolution occurs in this system largely on the basis of the change in molecular weight. The greater the amount of scission-induced molecular weight reduction the greater the solubility of the exposed resist in developers such as methyl ethylketone.

For resists based on exposure-induced functional group transformation such as in CARs, depending on their polarity and the polarity of the developer solvent, different types of interactions mediate the dissolution of the part that is dissolved in the developer. Positive-tone aqueous development of, for example, polar and charged CARs, have ionic interactions driven by highly polar polymer–polymer, hydration, and hydrogen bonding interactions, which decrease and break down the polymer–polymer interactions, making it easier for the water molecules of the developer to displace these interactions and solvate the charged polymeric units, ultimately dissolving them in the developer. In contrast, in negative-tone development in a nonpolar solvent of the above polar and charged CARs, the strong ionic polymer–polymer interactions, driven by polar hydrogen bonds of the exposed part of the film, make it much more difficult for solvent molecules to displace these interactions. Therefore, while the unexposed regions are readily developed away, the exposed polar region excludes solvent penetration, leading to high-contrast unswollen patterns.

## 2.7.5 Development rate characterization

There are several reasons why it is important to characterize the dissolution or development rate of any given resist. The main reasons tend to be for process control purposes, given that image discrimination in a resist is based on differences in dissolution rates between the image and non-image areas. The two main techniques that are used to characterize the dissolution properties of a resist are laser interferometry and quartz crystal microbalance. Each of these techniques is reviewed below.

### 2.7.5.1 Laser interferometry

The first use of laser interferometry in monitoring the dissolution rate of a resist during development was by Konnerth and Dill.<sup>182</sup> The basis of their idea is shown in Fig. 2.37. A laser beam is directed toward the film that is

<sup>182</sup>K. L. Konnerth and F. H. Dill, “In-situ measurement of dielectric thickness during etching or developing processes,” *IEEE Trans. Electron. Devices* **22**(7), 452–546 (1975); K. L. Konnerth and F. H. Dill, “IOTA, a new computer controlled thin film thickness measurement tool,” *Solid-State Electron.* **15**, 371 (1972).

They found that polymer dissolution occurs in two stages. In the first stage, solvent penetrates the glassy polymer, forming a gel layer that separates the polymer matrix from the pure solvent. In the second stage, the polymer coils disentangle from the gel, eventually diffusing into the liquid. Three distinct phases in the steady state dissolution process are<sup>196</sup>

Glassy polymer | Swollen gel | Solvent or solution

Ueberreiter found that, in the polymer systems he studied, the diffusion of the solvent across the gel layer is the rate-determining step (i.e., it is the slowest of all involved steps),<sup>197</sup> and in those cases solvent uptake and the inward movement of the glass–gel interface depend on the square root of time, as is characteristic of Fickian diffusion. In other systems, the processes in the glass–gel interface are rate determining, and solvent uptake and interface movement are linear functions of time. Alfrey, Gurnee, and Lloyd<sup>198</sup> termed this *case II diffusion* or polymer relaxation-controlled mass transfer.<sup>199</sup> Figure 2.40 shows a schematic of time–concentration profiles for the two dissolution modes.

In the following section, we discuss in some depth the dissolution mechanism of phenolic polymer resists such as novolac and PHOST resins, as well as those of acrylate and alicyclic resist polymer platforms. The development of phenolic polymer resins involves similar dissolution stages. Unlike their counterparts that are solvent developable—such as bis-azide/cis-polyisoprene negative resists, which require some degree of swelling for their dissolution—these phenolic polymer resists do not require such adverse swelling for dissolution.<sup>200</sup>

### 2.7.6.1 Dissolution mechanism of phenolic resists

The mechanism of phenolic polymer resist dissolution has been a hotly contested and debated concept. Many models have been proposed for how this process plays out. Although each of these models has been successful in explaining different aspects (but not the complete mechanism of novolac

<sup>196</sup>A. Reiser, *Photoreactive Polymers: The Science and Technology of Resists*, John Wiley & Sons, New York, p. 211 (1989).

<sup>197</sup>K. Ueberreiter, in *Diffusion in Polymers*, J. Crank and S. Park, Eds., Academic Press, New York (1968).

<sup>198</sup>T. Alfrey, Jr., E. F. Gurnee, and W. O. Lloyd, “Diffusion in glassy polymers,” *J. Polym. Sci., Part C* **12**, 249 (1960).

<sup>199</sup>G. C. Sarti, “Solvent osmotic stresses and the prediction of Case II transport kinetics,” *Polymer* **20**, 827 (1979); N. L. Thomas and A. H. Windle, “A theory of case II diffusion,” *Polymer* **23**, 529 (1982).

<sup>200</sup>J. P. Huang, T. K. Kwei, and A. Reiser, “Molecular mechanism of positive novolac resists,” *Proc. SPIE* **1086**, 74 (1989); H. Shih, T. Yeu, and A. Reiser, “Percolation view of novolac dissolution: 3. dissolution inhibition,” *Proc. SPIE* **2195**, 514 (1994); B. W. Smith, “Resist Processing,” in *Microlithography: Science and Technology*, J. R. Sheats and B. W. Smith, Eds., Marcel Dekker, Inc., p. 546 (1998).

$$\log\left(\frac{R}{R_1}\right) = -2\log(1 - p_c) + 2\log(p - p_c). \quad (2.44)$$

It is remarkable that these seven structurally different resins all yielded a slope of 2 on  $\log R$  vs.  $\log(p - p_c)$  plots for a value of  $p_c = 0.2$ ; all of them mapping perfectly onto the same master curve.<sup>251</sup> A major problem with the percolation model is that it predicts a resist contrast that is far lower than what is observed experimentally.

#### **2.7.6.1.3.5 Critical ionization model**

The critical ionization model proposed by Tsiartas et al.<sup>252</sup> states that a resist polymer below its entanglement molecular weight dissolves in a developer whenever a critical fraction of its blocked groups become deblocked. In the specific case of phenolic resins, dissolution proceeds via acid–base reaction between the aqueous developer base and the phenolic group of the resins, leading to deprotonation of the latter and formation of phenolate ions. Dissolution as a result occurs in the phenolic resins only when a critical fraction of the phenol groups in the polymer are ionized (deprotonated). Below this critical ionization fraction, no dissolution of the resin occurs in the developer. This implies that lower-molecular-weight polymers will require fewer deblocking (deprotonation or ionization) events to become soluble compared to their higher-molecular-weight counterparts.

#### **2.7.6.1.3.6 Stone wall model of novolac dissolution**

Proposed by Hanabata, Uetani, and Furuta<sup>253</sup> in 1990, the stone wall model states that during development, the low-molecular-weight novolacs and sensitizer (referred to as the mortar of the wall) in the exposed part of DNQ/novolac resist dissolve quickly; this has the effect of increasing the surface areas of the high-molecular-weight novolac (referred to as the “stones” of the wall) that is in contact with the developer, eventually leading to a breakup of the “stone wall,” and resulting in dissolution (see Fig. 2.50).

#### **2.7.6.1.3.7 Effects of resin and inhibitor structure on dissolution rate**

There is ample evidence that the structural properties of phenolic resins such as novolac and PHOST, as well as the inhibitors associated with them, do

<sup>251</sup>ibid.

<sup>252</sup>P. C. Tsiartas, L. W. Flanagan, C. L. Henderson, W. D. Hinsberg, I. C. Sanchez, R. T. Bonnacaze, and C. G. Willson, “The mechanism of phenolic polymer dissolution: A new perspective,” *Macromolecules* **30**(16), 4656–4664 (1996).

<sup>253</sup>M. Hanabata, Y. Uetani, and A. Furuta, “Novolac design for high resolution positive photoresists. II. Stone wall model for positive photoresist development,” *Proc. SPIE* **920**, 349–482 (1990).

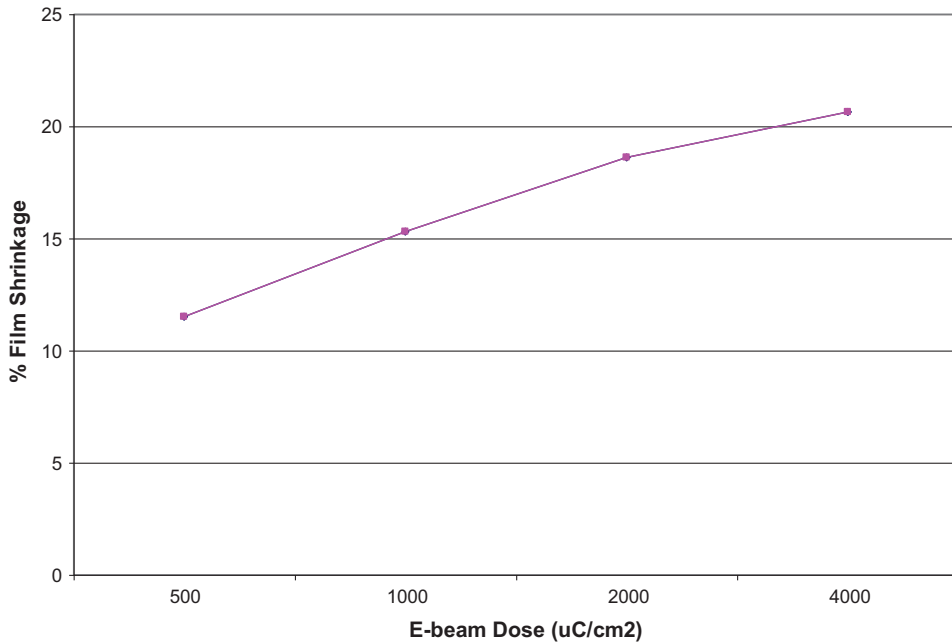


**Figure 2.59** Film shrinkage of PAR-700/A4 resist as a function of electron beam dose. The nominal resist thickness was 400 nm [reprinted from U. Okoroanyanwu, *Chemistry and Lithography*, SPIE Press, Bellingham, Washington p. 544 (2010)].

## 2.9 Resist Etching Chemistry

Following the resist pattern stabilization steps, an etching process is used to transfer the resist pattern into the underlying semiconductor substrate. There are two main forms of etching processes: wet and dry etching. Before the dry etching techniques were developed, all etching processes in semiconductor device fabrication were carried out with wet etching.

### 2.9.1 Wet etching

In wet etching, the substrate is etched with an etchant solution in a process that involves dipping the patterned resist wafer in the etchant solution and subsequently cleaning and rinsing it with pure de-ionized water. The wet etch rate is mainly dependent on the composition of the etchant solution and the temperature. Given that these two factors and the etching time are easily controllable, the reproducibility of the wet etch result is quite good.<sup>314</sup>

The choice of etchants depends on the nature of the substrate to be etched. Table 2.4 is a list of solutions used in the wet etching of common substrates. Silicon dioxide is etched with a mixture of aqueous solution of

<sup>314</sup>S. Nonogaki, T. Ueno, and T. Ito, *Microlithography Fundamentals in Semiconductor Devices & Fabrication Technology*, Marcel Dekker, Inc., New York, Chapter 5 (1998).

# Chapter 3

## Chemistry of the Lithographic Exposure Tool and Optical Element Materials

“And the atoms that compose this radiance do not travel as isolated individuals but linked and massed together.”  
Lucretius, *De Rerum Naturae* [*On the Nature of Things*]

### 3.1 Introduction

The optical elements of lithographic exposure tools comprise lenses, mirrors, reticles, and pellicles. The materials used in the fabrication of these optical elements are chosen because of their unique physical and chemical properties relative to their exposure wavelength of use.

### 3.2 Chemistry of Lens Materials

The main optical materials used in UV and visible light lithographic exposure tools fall into two categories: reflective optical materials (mirrors) and refractive optical materials (lenses). Reflective optical materials are advantageous because they can be used with broadband illumination. Also, it is very difficult to design and build high-numerical-aperture (NA) all-reflective optics because of physical interference: some mirrors will block the light path of others. For this reason, lithographic exposure tools utilizing all reflective optics such as production-worthy EUV exposure tools have low NA (0.33), with 0.55-NA systems currently under development. These tools achieve very high resolution because of their short exposure wavelength (13.5 nm). Deep-UV (DUV) lithographic tools have mostly lens-based optics and a few

shape of some stepper alignment signals.<sup>37</sup> Earlier generations of top anti-reflection coatings were designed to be coated from organic solvents that do not attack the resist layer and must be removed before development since they are not aqueous-base soluble. In principle, chlorofluorocarbons (CFCs) may be used for both purposes since they do not attack the resist.<sup>38</sup>

Inorganic anti-reflection coatings are typically deposited by sputtering, and, unlike organic anti-reflection coatings, may in some cases be left in the finished device. Typical inorganic anti-reflection coatings include silicon oxynitride, amorphous silicon, tantalum silicide, titanium nitride, etc.

### 3.3 Chemistry of Mirror Materials

#### 3.3.1 EUV multilayer mirrors

There are no reasonably EUV-transmissive refractive materials that can be used in EUV optics. Instead, most naturally occurring materials reflect only a very small fraction of the incident EUV photons and tend to absorb most of them from their surface within a fraction of a micron. Therefore, only precisely figured reflective optics, comprising multilayer film reflectors of alternating thin (a few nanometers) layers of molybdenum and silicon can be used as mirrors in the EUV tool. To protect the multilayer coating of the mirror, a capping layer is often deposited on its surface.

### 3.4 Chemistry of Lithographic Masks and Reticle Materials

There are two main types of optical lithographic masks: binary intensity masks (BIMs) and phase-shifting masks (PSMs). A BIM consists of a clear, transparent quartz substrate with uniform thickness, in which is embedded dark, opaque, non-transmitting patterns made of chromium, a chromium-containing compound layer, or a molybdenum-containing layer of approximately 80-nm in thickness.<sup>39</sup> Chromium and chromium-containing compounds are the most common opaque materials used for fabricating optical lithographic photomasks. Typically, the films of chromium and chromium-containing compounds are sputtered onto the glass substrates to thicknesses between 50 nm and 110 nm.<sup>40</sup> The optical constants of chromium at different lithographic wavelengths are given in Table 3.6. A consequence of the high absorption of chromium at the indicated lithographic wavelengths is

<sup>37</sup>T. Tanaka, N. Hasegawa, H. Shiraishi, and S. Okazaki, "A new photolithography technique with antireflective coating on resist ARCOR," *J. Electrochemical Society* **137**(12), 3900 (1990).

<sup>38</sup>Despite this quality, CFCs cannot be used as solvents for top anti-reflection coatings because they are now banned for their role in the depletion of the ozone layer.

<sup>39</sup>*ibid.*, p. 11.

<sup>40</sup>H. J. Levinson, *Principles of Lithography*, 2<sup>nd</sup> edition, SPIE Press, Bellingham, Washington, p. 247 (2005).

# Chapter 4

## Chemistry of Lithographic Patterning Materials

“Why is the grass so cool, fresh and green?  
The sky so deep, and blue?  
Get to your Chemistry,  
You dullard, you!”  
Walter de la Mare, “The Dunce”

### 4.1 Introduction

Present day lithographic patterning materials and chemicals, including inks, resists, anti-reflection coatings, casting solvents, developers, strippers, etc., evolved largely from technologies developed in the printing industry. Integrated circuits (ICs) and circuit boards were unheard of in 1798 when Senefelder invented lithography and in 1826 when Niepce invented photolithography. Since those early days, lithographic chemicals have evolved from being extracted from natural sources to being derived almost exclusively from synthetic sources today. They have also grown in importance along with the electronics industry, since even the simplest electronic systems today are patterned with resists, using ever more sophisticated arrays of lithographic chemicals. In this chapter we present an overview of lithographic chemicals used in patterning IC devices and printing newspapers, textbooks, posters and the like, while making historical references to similar materials used in lithography in earlier times.

### 4.2 Resists

As the enabling factor/component for each lithographic printing technique, resists have often determined the successful implementation of each lithography. At times, new resists and related processes developed in anticipation of yet-to-be developed lithographic tools and methods. Other times, the invention of



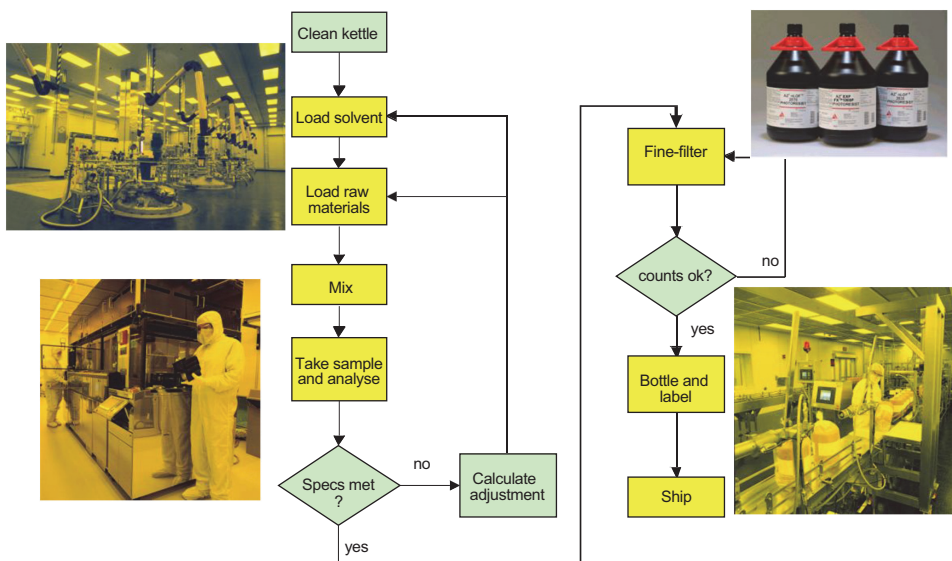


**Figure 4.13** Typical process flow for the large-scale manufacturing of advanced commercial resists (figure courtesy of R. Dammel).

appropriately to meet the specification. This iteration loop is executed as many times as necessary until the manufacturer's specification is met.

### 4.3 Resist Developers and Rinses

Resist developers fall into two main categories, depending on whether they are used for developing negative resists or positive resists. Negative resist developers are typically organic solvents in which the resist resins are soluble. Because the exposed area of the negative resist film is crosslinked and remains on the substrate, the unexposed part, still retaining the solubility characteristics of the parent resist resin, is dissolved away with the developing solvent. The actual negative resist development operation involves the selective dissolution of the unexposed areas. Chemically, the crosslinking caused by the exposure process does not significantly alter the resist polymer enough to prevent a strong interaction with solvents capable of dissolving the unexposed and uncrosslinked polymer. Consequently, swelling of the exposed areas will occur and can affect resist adhesion<sup>10</sup> if it is severe enough; it will continue until equilibrium is reached.<sup>11</sup> Ways to minimize the swelling problem of negative resists include applying adequate exposure to afford sufficient crosslinking, which in turn acts

<sup>10</sup>E. B. Davidson, in *Tech. Papers, Reg. Tech. Conf. Soc. Plast. Eng.*, Mid-Hudson Sec., p. 141, October (1970).

<sup>11</sup>W. S. DeForest, *Photoresist: Materials and Processes*, McGraw-Hill Book Company, New York, p. 242 (1975).

# Chapter 5

## Photochemistry and Radiation Chemistry in Lithography

“Mehr licht!” [More light!]

Attributed dying words of Johann Wolfgang von Goethe (1749–1832)

### 5.1 Introduction

Radiations spanning the visible, ultraviolet (UV), vacuum-UV (VUV), and extreme-UV (EUV) bands of the electromagnetic spectrum as well as charged particles such as electrons and ions are routinely used in semiconductor lithography. Photons with wavelengths from the visible (436 nm) through mid-UV (365 nm), deep-UV [(DUV) 248 nm and 193 nm], VUV (157 nm), and EUV (13.5 nm) regions of the spectrum are now routinely used in lithographic patterning of devices of different kinds. These photons mediate a wide range of photochemistry as they mediate the lithographic patterning process. Lithography using photons,<sup>1</sup> otherwise called photolithography or optical lithography, has been and continues to be the preeminent lithographic technique used in fabrication of integrated circuit devices in the semiconductor industry since the late 1950s. Figure 5.1 shows the six basic elements of an optical lithographic exposure tool through which these photons travel: (1) an exposure source, (2) an illumination optics system, (3) a photomask or reticle and its pellicle, (4) a projection optics system, (5) a wafer stage, and (6) a photoresist-coated wafer. The source provides the exposure radiation which, with the aid of illumination optics, illuminates the photomask and transfers the image of the

---

<sup>1</sup>The term *optical lithography* as used in this book encompasses all lithographic patterning techniques in which photons are used in such a manner that the imaging action obeys the laws of geometric optics—the simple laws of reflection and refraction, to mention but a few. With this usage, the terms photolithography and optical lithography are interchangeable, denoting the fact that photons are the primary agents that initiate the chemical transformations of the resists, resulting in the contrast between the exposed and the unexposed regions, and ultimately leading to the effective transfer of the mask image to the semiconducting substrate.

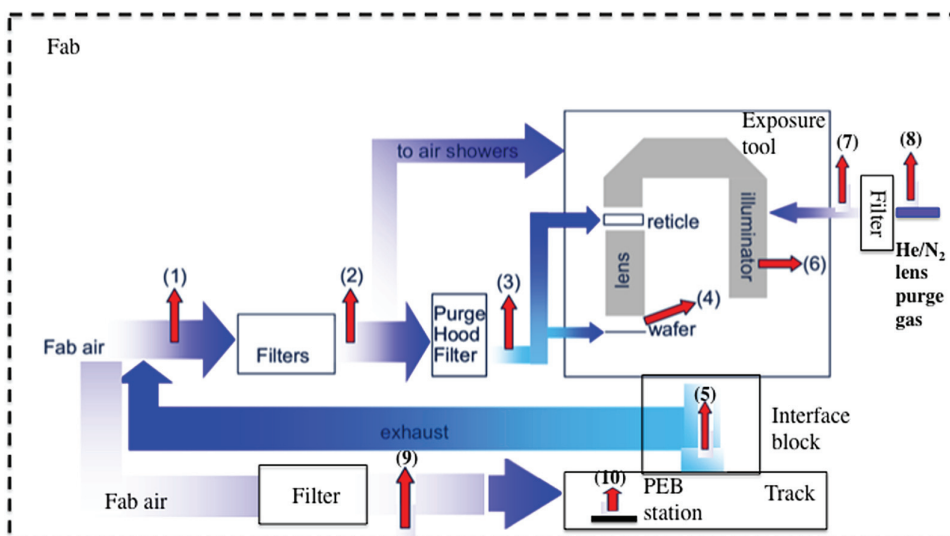


**Figure 5.2** Schematic representation of the air and lens purge gas flow through a typical lithographic exposure tool/track cluster, here illustrated with the ASML /1100 ArF lithographic exposure tool/Screen track cluster, and indicating locations used in airborne molecular contamination monitoring. Air and purge gas flows are indicated in blue color. Typical airborne molecular contamination monitoring locations are indicated with red arrows and are associated with numbers.

inspection, blank and patterned mask inspection, mask cleaning, and plasma stripping of resists from wafers and masks.

Distinct photochemical reactions and photophysical processes as well as radiochemical reactions and radiochemical processes are involved in the generation of radiation from lithographic exposure sources, and in the interaction of exposure radiation with lithographic optical elements, constituents of the exposure medium, and resist materials. These photochemical and radiochemical reactions and photophysical and radiochemical processes resulting from the interactions between the exposure radiation and radiation-sensitive resists and their constituents underlie the basis of the contrast between the exposed and the unexposed regions of the resist film. We examine some of these reactions and interactions in the succeeding sections.

## 5.2 General Considerations on Photochemistry, Photophysics, and Radiation Chemistry in Lithography

The interaction of the exposure radiation with the constituents of the exposure medium can generate reactive species that can degrade optical elements and the unexposed areas of the resist film. The interaction of the exposure radiation with the optical elements can equally degrade the latter. The introductory parts of some of the major sections of this chapter are therefore devoted to the

where  $\bar{\nu}_m$  is mean frequency of absorption in wavenumbers,  $\epsilon dv$  is experimental molar absorptivity integrated over the width of the absorption band, and  $\epsilon_{\max}$  is the maximum absorptivity within the absorption band.

The quantum yield is defined as the ratio of the number of excited molecules in each excited state (that decay by that process) to the total number of excited molecules in each state. The fluorescence and phosphorescence quantum yields are expressed as

$$\phi_F = \frac{\text{Rate of fluorescence emission}}{\text{Rate of excitation}} = \frac{k_F[S_1]}{I_A} \quad (5.33)$$

and

$$\phi_P = \frac{\text{Rate of phosphorescence emission}}{\text{Rate of excitation}} = \frac{k_P[T_1]}{I_A}, \quad (5.34)$$

respectively, where  $I_A$  is the rate of radiation absorption.

### 5.2.1.5 Types of electronic transitions in lithographic systems

Transitions in lithographic systems arise from the absorption of energy (in the form of electromagnetic radiation, electrical discharge, or chemical reactions) by a lithographic material, causing the movement of an electron from one molecular or atomic orbital of the material to another. The nature of the transition is described by the two orbitals involved. Typical transitions in lithography include (1) metal-centered  $d-d$  transitions between orbitals localized on transition metal atoms such as Sn used in laser-produced plasma for EUV lithography; (2) transitions between molecular orbitals in organic compounds and organometallic compounds in resists as well as in noble gas halides such as KrF and ArF exciplex laser sources; (3) transitions between the valence and conduction bands of impurity atoms that lead to color center formation in lithographic lenses made of quartz.

The lowest-energy transitions observed in lithographic systems are those between the highest occupied molecular orbital (HOMO) and lowest unoccupied molecular orbital (LUMO). The two most common types of transitions in organic molecules used in lithography (such as photoresists) include  $n \rightarrow \pi^*$  and  $\pi \rightarrow \pi^*$  transitions;  $\sigma \rightarrow \pi^*$  and  $\sigma \rightarrow \sigma^*$  transitions are usually of such high energy that they occur in the VUV region. Lithographic organic materials such as photoresists typically containing heteroatoms such as O and N have  $n \rightarrow \pi^*$  and  $\pi \rightarrow \pi^*$  transitions that are energetically close.

## 5.3 Radiation Chemistry versus Photochemistry in Lithography

Conventional photochemistry deals with valence or outer-shell electronic excitation associated with radiation lying in the approximate wavelength

the availability of an allylic hydrogen, substituent polymers react with it to produce either dioxetanes or hydroperoxides, whereas polydienes yield endoperoxides.<sup>119</sup> In polymers, light-absorbing impurities (external and/or internal structure irregularities) have been reported to act as potential photosensitizers for the generation of singlet oxygen.<sup>120</sup>

## 5.8 Photochemistry of Mask and Exposure Tool Lens Contamination and Cleaning

The exposure chamber of an optical lithographic tool is a veritable reaction vessel conducive to oxidative and etching reactions mediated by photoinduced species from the interaction of the exposure radiation with molecular contaminants in the exposure chamber on one hand, and between exposure radiation and mask materials on the other. These oxidation reactions ultimately lead to growth of inorganic salts such as ammonium sulfate and ammonium molybdate as well as carbon deposits on masks and exposure tool lenses. They can also lead to corrosion of the mask (discussed in Chapter 11), mediated via photoelectrochemical processes.

### 5.8.1 Inorganic salt formation on DUV exposure tool lenses and reticles

Experimental evidence suggests the formation of inorganic crystals that cause haze defects on 193-nm and 248-nm exposure reticles<sup>121</sup> and lenses. These

---

*Chem. Ed.* **14**, 463 (1976); J. F. Rabek and B. Ranby, "Studies on the photo-oxidative mechanism of polymers. VII. The role of singlet oxygen in the dye-photosensitized oxidation of cis-1,4- and 1,2-polybutadienes and butadiene-styrene copolymers," *J. Appl. Polym. Sci.* **23**, 2481 (1979); A. Zwiig and W. A. Henderson, "Singlet oxygen and polymer photooxidations. I. Sensitizers, quenchers, and reactants," *J. Polym. Sci. Chem. Ed.* **13**, 717 (1975).

<sup>119</sup>M. L. Kaplan and P. G. Kelleher, "Photo-oxidation of polymers without light: Oxidation of polybutadiene and an ABS polyblend with singlet oxygen," *J. Polym. Sci. Chem. Ed.* **8**, 3163 (1970); H. C. Ng and J. E. Guillet, "Singlet oxygen initiation of polymer photooxidation: photolysis of cis-1,4-poly(isoprene hydroperoxide)," *Macromolecules* **11**(5), 929 (1978); C. Tanielian and J. Chaineaux, "Single oxygen reactions with model compounds of cis and trans polyisoprene containing two units," *J. Photochem.* **9**, 19 (1978); C. Tanielian and J. Chaineaux, "Singlet oxygen reactions with model compounds of cis- and trans-polyisoprene containing one unit. Kinetic aspects," *J. Polym. Sci. Chem. Ed.* **17**, 715 (1979); C. Tanielian and J. Chaineaux, "Sensitized photo-oxidation of polyisoprene: effect of the presence of hydroxy and hydroperoxyl groups," *Europ. Polym. J.* **16**, 619 (1980).

<sup>120</sup>J. F. Rabek, *Photodegradation of Polymers: Physical Characteristics and Applications*, Springer, New York, p. 87 (1996).

<sup>121</sup>B. Grenon, K. Bhattacharyya, W. Volk, and A. Poock, "Reticle surface contaminants and their relationship to subpellicle particle formation," *Proc. SPIE* **5256** (2003); E. Johnstone, L. Dieu, C. Chovino, J. Reyes, D. Hong, P. Krishnan, D. Coburn, and C. Capella, "193-nm haze contamination: A close relationship between mask and its environment," *Proc. SPIE* **5256** (2003).

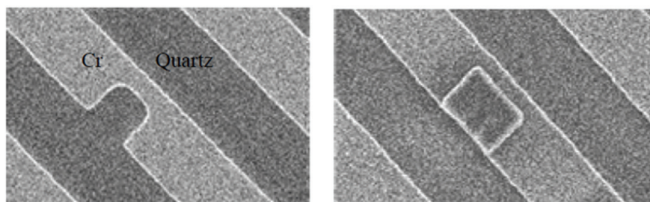
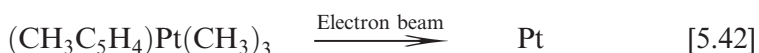


**Figure 5.37** Lithographic mask feature with clear defects (left) before electron beam-assisted Pt deposition and (right) after electron beam-assisted Pt deposition from a (methylcyclopentadienyl)platinum complex. (Reprinted from Liang et al.<sup>211</sup>)

before and after repair with this technique, illustrating the effectiveness of this approach in repairing such clear mask defects.<sup>211</sup>



## 5.11 Photochemistry and Radiation Chemistry of Resist Systems

### 5.11.1 Photochemistry of resist exposure

Figure 5.38 presents the main photochemical and radiochemical imaging mechanisms that underlie advanced lithography. There are two tones in photochemical and radiochemical resist imaging: negative and positive tone. For positive resists, the exposed part of the resist film is dissolved away during development, reproducing a positive image of the mask; in negative resists, the unexposed part the resist is dissolved away during development, leaving the exposed part, and reproducing a negative image of the mask. The photochemical and radiochemical reactions that engender negative-tone resist imaging mechanisms include photo- and radiation-initiated polymerization, crosslinking, and polarity switching reactions such as condensation, pinacol rearrangement, esterification, and ligand exchange. Negative-tone imaging mechanisms lead to either a significant increase in molecular weight of the exposed resist (as in polymerization and crosslinking imaging mechanisms), or polarity switching (as in condensation, pinacol rearrangement, esterification, and ligand exchange imaging mechanisms) of the exposed part of the resist relative to the unexposed part.

In contrast, the photochemical and radiochemical reactions that engender positive-tone resist imaging mechanisms include photolysis and radiolysis as well as radiation-induced main-chain scission and depolymerization.

<sup>211</sup>T. Liang, A. Stivers, M. Penn, D. Bald, C. Sethi, V. Boegli, M. Budach, K. Erdinger, and P. Spies, "Demonstration of damage-free mask repair using electron beam-induced processes," *Proc. SPIE* **5446**, (2004).

### 5.11.5.4 Determination of the crosslinking yield $G_x$

In the absence of scissioning, the radiation chemical yield of crosslinking<sup>309</sup> is readily determined by monitoring the insolubilization of the polymer. Charlesby and Pinner<sup>310</sup> show that the soluble fraction  $s$  as a function of the irradiation dose received by the polymer can be described by an equation of the form

$$s + s^{1/2} = \frac{G_s}{2G_x} + \frac{9.65 \times 10^5}{M_n^0 G_x} \frac{1}{D}. \quad (5.72)$$

In the procedure, the polymer sample is irradiated and then extracted with a suitable solvent, in which the soluble fraction (i.e., the fraction of the material that is not crosslinked) can be determined. A plot of  $(s + s^{1/2})$  against  $1/D$  yields a straight line from which the value of  $G_x$  can be determined from either the intercept or the slope.

In a polymer in which both crosslinking and backbone scission are occurring to a significant degree, the  $G$ -values of both processes can be derived simultaneously by measuring the number-average and weight-average molecular weights,  $M_n$  and  $M_w$ , respectively, of the sample under irradiation. The  $M_n$  and  $M_w$  values can be expressed by two equations of similar form:

$$\frac{1}{M_n} = \frac{1}{M_n^0} + [G_s - G_x] \frac{D}{100N_A}, \quad (5.73)$$

$$\frac{1}{M_w} = \frac{1}{M_w^0} + [G_s - 4G_x] \frac{D}{100N_A}. \quad (5.74)$$

A plot of the reciprocal molecular weight of the sample as a function of radiation dose yields straight lines, from which slope the values of  $[G_s - G_x]$  and  $[G_s - 4G_x]$  can be obtained to yield the  $G$ -values.

### 5.11.6 Photochemistry of photoactive compounds

There are three classes of photoactive compounds used in lithography: photoacids, photobases, and photosensitizers. We briefly describe here their photochemistry.<sup>311</sup> In Chapters 6 and 7, we discuss their lithographic

<sup>309</sup>The method presented here is adapted from the treatment of the subject given in A. Reiser, *Photoreactive Polymers: The Science and Technology of Resists*, John Wiley & Sons, New York, pp. 309–311 (1989).

<sup>310</sup>A. Charlesby and S. H. Pinner, "Analysis of the solubility of irradiated polyethylene and other polymers," *Proc. R. Soc. London, Ser. A* **249**, 367 (1959).

<sup>311</sup>Excellent reviews of the photochemistry of these compounds have been published; the analysis here is drawn largely from M. Shirai and M. Tsunooka, "Photoacid and photobase generators: chemistry and applications to polymeric materials," *Prog. Polym. Sci.* **21**, 1–46 (1986); C. J. Martin, G. Rapenne, T. Nakashima, and T. Kawai, "Recent progress in development of photoacid generators," *J. Photochem. Photobiol. C: Photochem. Reviews* **34**, 41–51 (2018).

# Chapter 6

## Chemistry of Photochemical and Radiochemical Imaging Mechanisms of Negative-Tone Resists

“...How charming it would be if it were possible to cause these natural images to imprint themselves durably and remain fixed upon the paper! And why should it not be possible? I asked myself.”

William Henry Fox Talbot, *The Pencil of Nature*

### 6.1 Introduction

As discussed in Chapter 4, resists in use before the 1960s were all invariably negative resists. These included resist materials such as bitumen of Judea, dichromated gelatin, and other dichromated colloids. The mechanism by which they functioned was not well understood at the time of their discovery. It was only in the 1920s that it was recognized that gelatin and other natural colloids were macromolecules<sup>1</sup> and that rubber vulcanization is a crosslinking process. Only then did the idea begin to take hold that the hardening and insolubilization that occur on exposure of dichromated gelatin are brought about by radiation-induced crosslinking.<sup>2</sup>

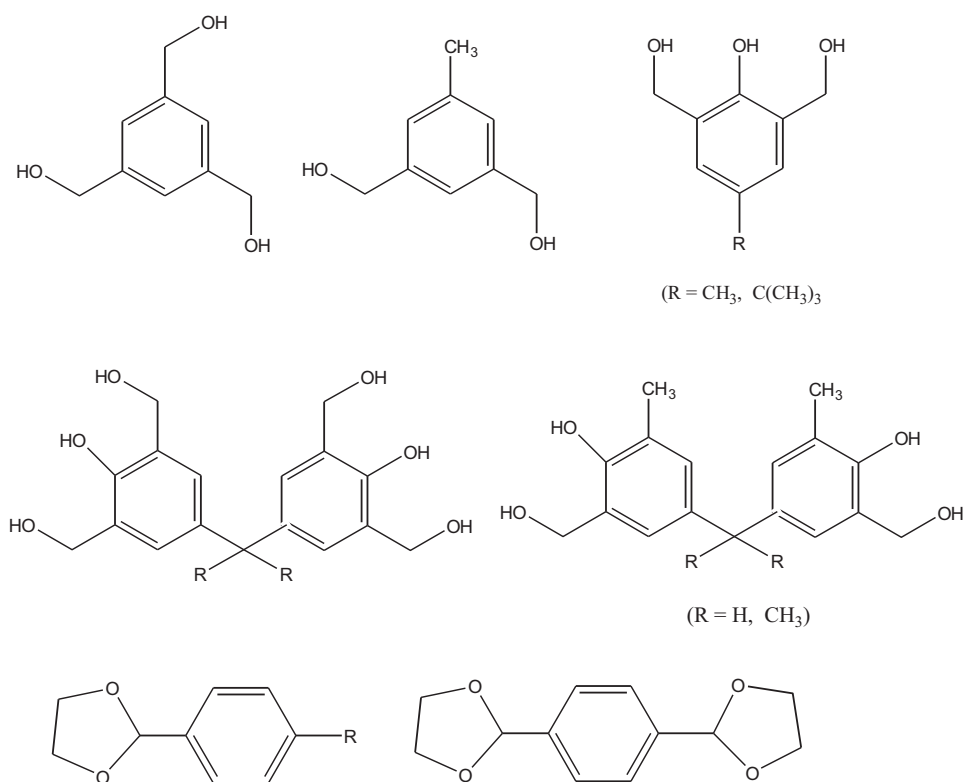
Characteristically, negative resists of the modern era (since 1950) have high chemical resistance and good image reproduction qualities. They were widely used in the manufacture of circuit boards and microelectronic devices for these reasons before the advent of positive resists. Because of their high chemical

<sup>1</sup>H. Morawetz, “Difficulties in the emergence of the polymer concept – an essay,” *Angewandte Chem. Int. Ed. Engl.* **26**, 93 (1987).

<sup>2</sup>A. Reiser, *Photoreactive Polymers: The Science and Technology of Resists*, John Wiley & Sons, New York, p. 22 (1989).



by selective removal of the *t*-BOC group in refluxing glacial acetic acid, to afford a copolymer bearing both the latent electrophile and the crosslinking site on the same polymer chain.<sup>138</sup> The formation of carbocation from the protonated ether moiety is the rate-determining step for crosslinking in these resists. Both the *C*-alkylation and *O*-alkylation are responsible for crosslinking and result in the destruction of the base-solubilizing phenolic OH groups in the exposed areas of the film, and hence negative-tone imaging. These condensation negative resists have found widespread application in DUV 248-nm, electron-beam, and x-ray lithographies, where they have provided excellent lithographic performance.<sup>139</sup>



(XXV) Examples of latent electrophiles (crosslinkers)

### 6.3.2.2 Negative resists based on radiation-induced polarity changes

Radiation-induced changes in the polarity of inorganic compounds or molecules or polymer-bound functional groups can significantly alter the

<sup>138</sup>ibid., p. 156.

<sup>139</sup>ibid., pp. 152–156.

dissolution properties of the polymer.<sup>140</sup> This idea has been used widely in the design of a very important class of negative resists, spanning both photolithography and charged-particle lithography. The most prominent examples of non-chemically amplified resists and chemically amplified resists are illustrated below. We follow the approaches reported by D. A. Doane and A. Heller<sup>141</sup> for the non-chemically amplified resists, and the approaches reported by both Reiser<sup>142</sup> and Ito<sup>143</sup> for the chemically amplified resists.

### **6.3.2.2.1 Non-chemically amplified negative resists based on radiation-induced polarity changes**

#### **6.3.2.2.1.1 Metal-chalcogenide resists**

Metal-chalcogenide inorganic resists are based on a photodoping phenomenon occurring in chalcogenide glass films, a phenomenon first reported in 1966 by M. T. Kostyshin and coworkers,<sup>144</sup> who showed that chalcogenide films deposited on metal substrates produce visible images upon UV irradiation. It was Shimizu et al.<sup>145</sup> who were the first group to extensively study various metal-chalcogenide systems as imaging materials; they introduced the term “photodoping” in 1971 to refer to the migration of a

---

<sup>140</sup>The classical example of radiation-induced polarity change is the photodecomposition of diazoquinone into an ionizable compound, the indene carboxylic acid. This reaction is the basis of one of the important positive photoresists discussed in Chapter 7. Attaching diazoquinone units to a polymer backbone, for example, via acrylic side groups, makes the unexposed polymer soluble in organic solvents and the exposed polymer soluble in dilute aqueous basic solutions.

<sup>141</sup>D. A. Doane and A. Heller, Eds., *Proc. Symposium on Inorganic Resist Systems* **82-9**, The Electrochemical Society, Pennington, New Jersey (1982).

<sup>142</sup>A. Reiser, *Photoactive Polymers: The Science and Technology of Resists*, John Wiley & Sons, New York, pp. 44–46 (1989).

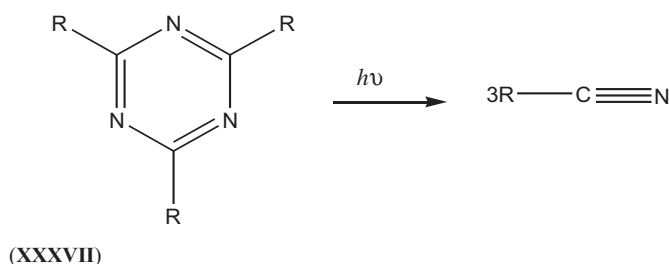
<sup>143</sup>H. Ito, *Chemical Amplification Resists for Microlithography*, *Adv. Polym. Sci.* **172**, Springer-Verlag, Berlin, pp. 149–174 (2005).

<sup>144</sup>The original papers by Kostyshin and co-workers can be found as M. T. Kostyshin, E. V. Mikhailovskaya, and P. F. Romanenko, “Photographic sensitivity effect in thin semiconducting films on metal substrates,” *Soviet Phys.-Solid-State* **8**, 451 (1966) [see, for example, D. A. Doane and A. Heller, “An introductory perspective on inorganic resist systems,” in *Proc. Symposium on Inorganic Resist Systems* **82-9**, D. A. Doane and A. Heller, Eds., The Electrochemical Society, Pennington, New Jersey (1982)].

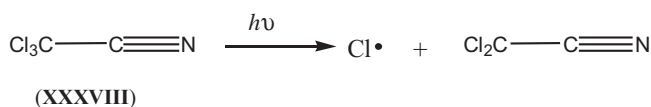
<sup>145</sup>I. Shimizu, H. Sakuma, H. Kokado, and E. Inoue, “The photo-doping of metals into solids for new-type imaging systems,” *Bull. Chem. Soc. Jap.* **44**, 1173 (1971); H. Kokado, I. Shimizu, and E. Inoue, “Discussion on the mechanism of photodoping,” *J. Non-cryst. Sol.* **20**, 131 (1976); I. Shimizu, H. Sakuma, H. Kokado, and E. Inoue, “Metal-chalcogenides systems as imaging materials,” *Photogr. Sci. Eng.* **16**, 291 (1972); I. Shimizu, H. Sakuma, H. Kokado, and E. Inoue, “The optical and electrical properties of metal photodoped chalcogenide glasses,” *Bull. Chem. Soc. Jap.* **46**, 1291 (1973); T. Shirakawa, I. Shimizu, H. Kokado, and E. Inoue, “Relief image in Ag-chalcogenide glass sensors,” *Photogr. Sci. Eng.* **19**, 139 (1975).

#### 6.6.1.1.2.4 Triazines

Triazines (**XXXVII**) are a class of symmetrical initiators that fragment; upon excitation, they dissociate into three substituted nitriles (**XXXVIII**) (Scheme 6.42).<sup>270</sup> Specifically, the primary photoproducts are not radicals, but they dissociate into radicals in a secondary thermal step (Scheme 6.43).<sup>271</sup>



**Scheme 6.42** Photodecomposition of triazine



**Scheme 6.43** Photodecomposition of nitriles

### 6.6.2 Radicals generated by hydrogen abstraction

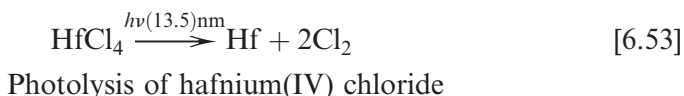
Abstraction of hydrogen by excited-state molecules makes possible the generation of radicals from molecules with low excitation energies, which effectively extends photoionization (that can initiate photopolymerization of reactive monomers) into the visible part of the spectrum. Examples of H-abstraction reactions include those by the excited triplet states of ketones like anthraquinone (**XXXVIX**). Photoirradiation of anthraquinone, for instance, in the hydrogen donor solvent tetrahydrofuran (THF) leads to the following processes (Scheme 6.44).<sup>272</sup>

In the presence of a reactive monomer, the radicals formed by the hydrogen abstraction initiate chain polymerization. However, in the absence of any other reactive species, the radicals can combine to form dimers. The species that absorbs the radiation (anthraquinone) and gets promoted to an

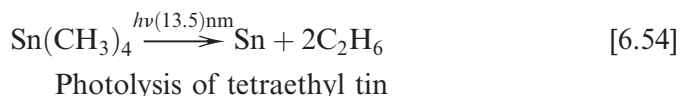
<sup>270</sup>H. Sakuraji, M. Yoshida, H. Kinoshita, K. Utena, K. Tokumaru, and M. Yoshiro, "Structure-reactivity relationships in triplet sensitized photolysis of aromatic ketone O-acyloximes," *Tetrahedron Lett.* **20**, p. 1529 (1978).

<sup>271</sup>A. Reiser, *Photoactive Polymers: The Science and Technology of Resists*, John Wiley & Sons, New York, p. 113 (1989).

<sup>272</sup>*ibid.*, pp. 113–114.



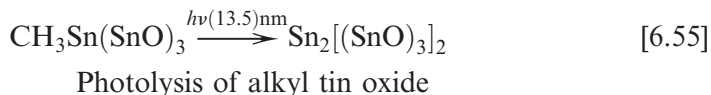
Tetraethyl tin is photodecomposed to metallic tin and ethane gas:



The final step is the dry development of the EUV-patterned film. The substrate is transferred outside the vacuum ambient of the EUV tool before development is performed. Development involves heating the substrate to volatilize the unexposed region, leaving behind the exposed metallic mask. Following lithographic patterning, pattern transfer to the underlying substrate is the same as in the conventional hard-mask-etch process.

Another variation of Lam's metal organic EUV resist process involves the CVD deposition of photosensitive metal oxide films such as organotin oxide from the reaction of suitable precursors and  $\text{CO}_2$  in a RF plasma. Potential precursors could include, for example, halo alkyltin, alkoxyalkyltin, or amidoalkyltin, with specific examples including trimethyltin chloride, dimethyltin dichloride, methyltin trichloride, tris(dimethylamino)methyltin(IV), and (dimethylamino)trimethyltin(IV).<sup>345</sup>

Following the deposition of the photosensitive metal oxide film, the film-coated substrate is transferred under vacuum to an EUV exposure tool for patterning. Upon EUV exposure, the organotin oxide dimerizes in the exposed region of the film, inducing a chemical contrast between the exposed and unexposed areas (Reaction 6.55).



Development involves contacting the exposed film with hot ethanol solution, which removes the unexposed area, leaving behind the metal oxide.

## 6.10 Lithographic Applications of Photopolymerization Negative Resists

Photoinitiated polymerization in negative resists used in lithography has found its main applications in lithographic offset plates in dry resists used in the printing of wire boards, printed circuit boards, solder masks, etc. Other emerging applications of this class of resists are in thick film imaging for MEMS applications as well as in 3D lithography, which is often referred to as

<sup>345</sup>D. Smith and D. M. Hausmann, "EUV photopatterning of vapor-deposited metal oxide-containing hardmasks," U.S. Patent No. 9,996,004 (2018).

# Chapter 7

## Chemistry of Photochemical and Radiochemical Imaging Mechanisms of Positive-Tone Resists

“... and may not bodies receive much of their activity from the particles of light which enter into their composition?”

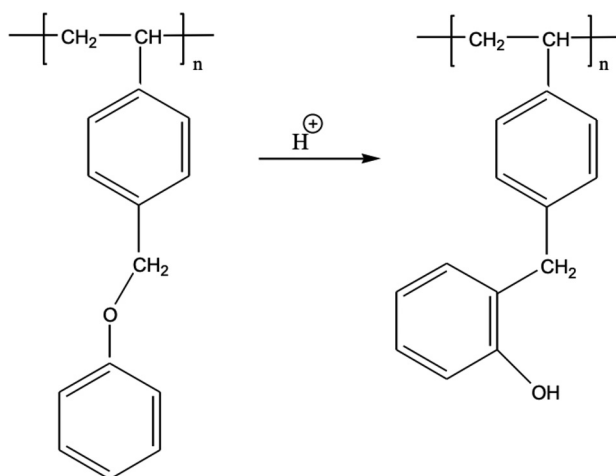
Isaac Newton, *Opticks*

### 7.1 Introduction

The essential characteristic of a positive resist is that its exposed part gets dissolved away in a developer solution, while its unexposed part does not. Positive resists differ from their negative counterparts principally in their response to actinic radiation despite the fact that the essential compositions of the two resist types are similar in many ways: each contains sensitizers or appropriate radiation-sensitive compounds, resins, solvents, and additives. As in modern negative resists, the resins for positive resists are polymers, which are large molecules with repetitive sequences of monomers—groups of atoms—connected in a linear or branched fashion, as illustrated in Fig. 4.3. The physical, thermal, mechanical, and molecular weight properties of lithographic polymers are discussed in Chapter 4. Unlike some negative resists, positive resists do not swell in developer. Moreover, the use of aqueous stripping and developing solutions greatly simplifies the equipment selection for positive resists in process equipment tooling by allowing low-cost, readily available plastics to be used as containers. Problems associated with the use of flammable solvents are minimized with positive resists.<sup>1</sup>

---

<sup>1</sup>W. S. Deforest, *Photoresist Materials and Processes*, McGraw-Hill, New York, p. 47 (1975).



**Scheme 7.44** Acid-catalyzed Claisen rearrangement of poly(4-phenoxyethyl styrene)

transformation, the resist polymer changes from the nonpolar to the polar state. Poly(4-phenoxyethyl styrene) is isomerized in a similar manner with an acid as a catalyst to a C-alkylated phenolic structure (Scheme 7.44).<sup>343</sup>

#### 7.2.2.2.1.3 Chemically amplified positive resists based on depolymerization

**Poly(phthalaldehyde) resists.** Unaware of the first patent granted for a CAR (granted to 3M Corporation), C. G. Willson, J. M. J. Fréchet, and H. Ito set out in the late 1970s to develop chemically amplified DUV resists. Their first attempt,<sup>344</sup> which was the second CAR invented for use in lithographic resist applications, involved the use of poly(phthalaldehyde), which undergoes an equilibrium cyclopolymerization and has a ceiling temperature of about  $-40$  °C. Their idea was to prepare the polymer below its ceiling temperature, then cap it and isolate the intrinsically unstable product. Reasoning that any photochemical event that can generate the anionic chain end above the ceiling temperature should cause spontaneous depolymerization to the monomer, they prepared the polymer by anionic copolymerization of phthalaldehyde and *o*-nitrobenzaldehyde monomers and capped it with acylating agents. They incorporated *o*-nitrobenzaldehyde as a monomer into the polymer to render it photosensitive. Exposing the films of the capped copolymer to DUV radiation resulted in spontaneous relief image formation, but the resulting images could

<sup>343</sup>H. Ito, *Chemical Amplification Resists for Microlithography*, *Adv. Polym. Sci.* **173**, Springer-Verlag, Berlin, p. 148 (2005).

<sup>344</sup>This is the second CAR invented for use in semiconductor lithography. Invented by Willson, Fréchet, and Ito, the resist upon exposure spontaneously and uncontrollably depolymerizes in an exothermic reaction that is sufficiently energetic to evaporate the monomer. These inventors were unaware of the 3M Corporation's patent on a similar concept (G. H. Smith and J. A. Bonham, U.S. Patent No. 3779,778 (1973)).

# Chapter 8

## Chemistry of the Limiting Issues of Photochemical and Radiochemical Resists and Approaches to Their Solutions

“In Nature’s infinite book of secrecy a little can I read.”

William Shakespeare, *Antony and Cleopatra*

### 8.1 Introduction

As shrinking integrated circuit (IC) device dimensions, fueled by the need to increase device speed and density, approach dimensions considerably smaller than the practical resolution limit of conventional lithography, several advanced resist processing schemes have been proposed to accommodate the resolution requirements for IC devices at such extremely small technology nodes. These processing schemes were introduced at the 32-nm technology node and were extended to the 22-nm technology node; they have now become firmly established at the sub-22-nm technology nodes of 15 nm, 10 nm, and 7 nm, patterned with immersion ArF and EUV lithography. With the successful implementation of EUV lithography in manufacturing at the 10-nm and 7-nm technology nodes, patterning challenges have shifted from resolution to noise, sensitivity, overlay, and edge placement. Of these challenges, the materials-related issues are sensitivity and noise. Noise in this instance is the natural variation in lithographic pattern placement, shape, and size. It causes line edge roughness, linewidth variation, and stochastic defects. This noise is ultimately due to the random nature of discrete photon events, electron events, molecular positions, and molecular quantities involved in the radiation-based lithographic exposure patterning process. It equally determines the ultimate critical dimension uniformity obtainable with any given radiation-based lithographic exposure process.

### 8.3.2 Resolution limits due to confinement effects in resists

Resist technologies that will enable EUV lithographic patterning at the sub-22-nm technology nodes must be capable of exceptional CD control, in addition to having low LER. Given the significant attenuation of EUV radiation in organic materials, ultrathin resist (thickness  $\leq 100$  nm) imaging appears to be the only viable option for single-exposure patterning at the sub-22-nm technology nodes. The 2008 ITRS specifications call for a resist thickness of 35–65 nm for the 22-nm technology node. However, the stability of ultrathin resist (UTR) films presents very difficult challenges due primarily to confinement effects. In addition, UTR imaging will require materials (resists and underlayers such as hard masks) with superb etch selectivity and etch processes that lead to negligible roughness transfer between layer stacks.

As discussed in Chapter 1, experimental results suggest that material properties of UTR films can differ in significant ways from their bulk counterparts. Of particular interest, because of its influence on the viscoelastic behavior of spin-coated films, is the effect of film thickness on the glass transition temperature  $T_g$  (see Fig. 8.18). The  $T_g$  decreases with film thickness for the substrate investigated in the study.

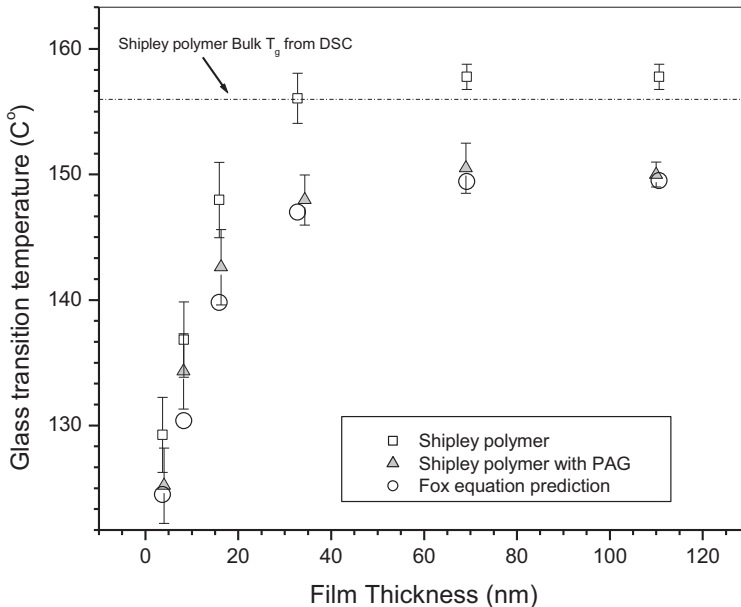


**Figure 8.18** Glass transition temperature of a resist polymer and a resist polymer with PAG as a function of film thickness (reprinted from D'Amour, Frank, and Okoroanyanwu<sup>53</sup>).

<sup>53</sup>J. N. D'Amour, C. W. Frank, and U. Okoroanyanwu, "Measuring thermophysical properties of ultrathin photoresist films," *Proc. SPIE* **4690**, 936–942 (2002); J. D'Amour, C. W. Frank, and U. Okoroanyanwu, "Modification to thermophysical behavior in ultrathin polymer films," *Proc. SPIE* **5039**, 996–1007 (2003).



electrons of the metals. Further, the high EUV absorptivity of these metallic hard mask resists enhances their photosensitivity to EUV exposure.

### **8.5 Resist Materials Outlook for the Advanced Technology Nodes**

It is expected that EUV lithography would be used to pattern devices at the advanced technology nodes of 5 nm, 3 nm, and 1.5 nm. To support patterning at these nodes, research efforts should be devoted to developing: (1) high-NA resist concepts beyond CARS that involve high-absorbance materials, including resists and underlayers, and development of new contrast mechanisms for high-NA EUV lithography; and (2) positive-tone metal containing resists or other resist concepts. Resists based on the condensation mechanism of metal oxo-hydroxo networks with organic and peroxy ligands, formulated from clusters with uniform molecular weights, appear to be promising candidates for these applications.

The chemical amplification concept has served the lithographic community well over many technology nodes. It still has a lot to give but is almost operating at its limits. Image blur caused by acid diffusion into unexposed areas of resists can only be limited, but not eliminated, if high sensitivity due to chemical amplification is to be maintained. This is because the mechanisms responsible for high sensitivity in CARs are intimately tied to the processes that lead to image blurring. This makes it extremely difficult, if not impossible, to strike the right resolution–LER–sensitivity trade-off balance with CARs based on the conventional design concepts. To this end, novel resist design concepts such as the multi-trigger resist concept and the photosensitization chemical amplification concept (both discussed above) are gaining traction within the semiconductor industry. So far, both techniques have demonstrated promising performance results with respect to meeting the resolution–LER–sensitivity target for some of the advanced technology nodes. In addition, the development of vapor deposited, dry developed metallic hard mask resists offers significant opportunities for improving sensitivity, LER, and linewidth variation.

Other new resist design concepts incorporating different polymer architectures and PAGs that can achieve high sensitivity are currently under serious exploration. Such alternative resist design concepts could incorporate photocatalysts with well-defined limited lifetimes, whose diffusion length at a nominal processing temperature could be targeted to match the resolution requirements at advanced technology node design rules. This will ensure that, at the barest minimum, the acid can only diffuse to a manageable distance that should fall within the geometry of the given advanced technology node design rules.

# Chapter 9

## Chemistry of Self-Assembling Lithographic Imaging Mechanisms

“The cause is hidden. The effect is visible to all.”  
Publius Ovidus Nasso [Ovid]

### 9.1 Introduction

Lithography based on self-assembly exploits the thermodynamic drive of certain systems such as block copolymers,<sup>1</sup> colloidal particles, and monolayers to spontaneously self-assemble into ordered structures. Three main variants of this phenomenon are exploited in lithography: block copolymer self-assembly, colloidal particle self-assembly, and monolayer self-assembly. Of these three variants of directed self-assembly (DSA) phenomena, directed block copolymer self-assembly is the one that has generated most interest in the semiconductor industry, where it is seen as a potential technology for complementary patterning to traditional radiation-based lithographic techniques in advanced technology nodes.<sup>2</sup> It is a patterning technique capable of pitch reduction and

---

<sup>1</sup>A detailed treatment of the theory of block copolymer self-assembly lithographic imaging mechanisms has been provided elsewhere; see, for example, U. Okoroanyanwu, *Molecular Theory of Lithography*, SPIE Press, Bellingham, Washington, Chapter 5 (2015). We highlight here essential chemical aspects of this theory, drawn largely from the above reference. We also examine the chemical aspects of a variety of strategies employed in lithographically directed block copolymer self-assembly, monomolecular-layer self-assembly lithography, and colloidal particle self-assembly lithography.

<sup>2</sup>K. Lai, C.-C. Liu, H. Tsai, Y. Xu, C. Chi, A. Raghunathan, P. Dhagat, L. Hu, O. Park, S. Jung, W. Cho, J. Morillo, J. Pitera, K. Schimdt, M. Guillorn, M. Brink, D. Sanders, N. Felix, T. Bailey, and M. Colburn, “Design technology co-optimization assessment for directed self-assembly-based lithography: Design for directed self-assembly or directed self-assembly for design?” *J. MicrolNanolith. MEMS MOEMS* **16**(1), 013502 (2017); R. Tiron, A. Gharbi,

## 9.2.2 Block copolymer synthesis via controlled radical polymerization

The strategy underlying controlled radical polymerization is to establish a dynamic equilibrium between a small fraction of growing free radicals and a large majority of dormant species, while eliminating or suppressing undesired termination and chain transfer reactions.<sup>172</sup> Such a dynamic and rapid equilibrium permits an equal opportunity for all growing or dormant chains to propagate via the frequent interconversion between the active and dormant species, leading to nearly uniform chains with narrow molecular-weight distribution. This technique reduces the rate of radical recombination by lowering the effective concentration of radicals.

The polymerization mechanism in controlled radical polymerization comprises: the initiation step, where the initiating radicals are formed via homolytic or heterolytic cleavage of the initiator into radicals, followed by addition of the radical across the double bond of the monomer; the propagation step, in which the monomers successively insert into the bond between the growing chain end and the radical; and the chain termination, where radicals combine with each other to form stable species. The propagation and termination of the generated free radicals proceed as in conventional radical polymerization, although the presence of a small fraction of radicals prevents premature termination.

The two main types of controlled radical polymerization techniques currently in use are: (1) stable free-radical polymerization (SFRP), involving the use of stable free-radicals such as nitroxides as reversible terminating agents to control the polymerization process,<sup>173,174</sup> and (2) atom transfer polymerization (ATRP).

As the living radical polymerization mechanism involves propagation through radicals, considerations involving monomer purity and reactivity in conjunction with relative rates of crossover and propagation reactions for the second monomer are factored into the overall sequential monomer addition synthetic strategy. The intermediate product formed after the polymerization of the first monomer must be able to initiate the polymerization of the second monomer. Often, this may require the purification of the intermediate product to eliminate all traces of the first monomer. Furthermore, if purification of the intermediate product is not done, statistical copolymerization of the second block may occur.

### 9.2.2.1 Block copolymers synthesis via atom transfer polymerization (ATRP)

In the ATRP technique, radicals are generated through a reversible redox process, catalyzed by transition metal complexes of Cu, Ru, Fe, Ni, Rh, or Pd, such as, for example, CuX/bipyridine, that undergo a one-electron

<sup>172</sup>K. Matyjaszewski, "Mechanistic Aspects of Atom Transfer Radical Polymerization," in *Controlled Free Radical Polymerization*, K. Matyjaszewski, Ed., *ACS Symposium Series* **685**, American Chemical Society, Washington, D.C., pp. 258–283 (1998).

<sup>173</sup>G. Moad, E. Rizzardo, and D. H. Solomon, "Selectivity of the reaction of free radicals with styrene," *Macromolecules* **15**, 909 (1982).

<sup>174</sup>M. K. Georges, R. P. N. Veregin, P. M. Kazmaier, and G. K. Hamer, "Narrow molecular weight resins by a free-radical polymerization process," *Macromolecules* **26**, 2987 (1993).

#### 9.2.6.4.5 Soft lithography

In the soft lithography method, resist is imprinted with a PDMS stamp to create grating patterns, following which a BCP film is spin-coated onto the space between the gratings to template the location of copolymer domains, which in turn self-assemble and align parallel to the gratings in an orientation perpendicular to the substrate.<sup>301</sup>

#### 9.2.7 Scaling block copolymer domain periodicity

As described above, the BCP composition determines the block domain periodicity or pitch  $L_0$ , and by extension, the CDs that are patternable with the BCP; other factors that determine the block domain periodicity include the domain orientation and the overall pattern formation process. The directly controllable primary physical parameters are monomer type, compositional ratio, molecular weight, and polydispersity, as well as the purity of the BCP and the Flory–Huggins interaction parameter  $\chi$ . The periodicity is related to the polymer chain length  $L_0$ , which in turn is related to the total degree of polymerization for each block. This implies that the length of each block, as controlled by the number of monomers in the block, is the determinant factor for the periodicity of the domain. Figure 9.14 illustrates how a BCP assembles to form the defined CD within the two guide parameters. Two polymer chains with similar ends interact to define the CD, shown as either blue or red domains. Because the two blocks have different polarities, phase separation ensures that the two ends of the BCP must have similar polarities to interact with each other. Thus, the two blue ends of the BCP in Fig. 9.14 must interact with each other.<sup>302</sup>

Polydispersity of the blocks of the BCP, a measure of the distribution of the molecular weight, plays a critical role in determining the uniformity or variability of domain pitch and CD uniformity. BCPs with blocks of unity monodispersity that have uniform chain lengths will yield more-uniform domain pitches and CDs, while BCPs with blocks that are polydispersed with polymer chains that are not of a uniform length will yield less-uniform domain pitches and CDs, and will also be more prone to imperfections during the self-assembly process.

A major factor that affects domain spacing is the ability of each block in the BCP to segregate into its own domain. The interaction parameter  $\chi$  is a major determinant of this ability to self-segregate away from the other block. The stronger the interaction parameter  $\chi$  between the blocks the easier it is for the two chains to assemble into their own domains, even when the chains are

<sup>301</sup>L. Li and H. Yokoyama, “Aligning single-layer cylinders of block copolymer nanodomains using soft molding,” *Adv. Mater.* **17**, 1432–1436 (2005).

<sup>302</sup>D. J. Guerrero, “A lithographer’s guide to patterning CMOS devices with directed self-assembly,” *Spotlight Series*, SPIE Press, Bellingham, Washington, p. 4 (2020).

# Chapter 10

## Chemistry of Imprint Lithographic Imaging Mechanisms

“A small rock holds back a great wave.”

Homer, *The Odyssey*

### 10.1 Introduction

Imprint lithography, invented by Chou and co-workers,<sup>1</sup> is a  $1\times$  printing technique based on the principle of mechanical deformation of a thin thermoplastic polymeric film (in the case of thermal imprint lithography) or photocurable resist liquid film, comprising monomers, oligomers, additives, and initiators (in the case of UV imprint lithography), brought about by directly pressing the resist with a template/mold/stamp containing a negative of the pattern of the features to be printed such that the resist flows and fills the open areas of the mold, replicating the desired pattern. As its imaging mechanism is not mediated by photons or charged beam particles such as electrons or ions, which suffer from diffraction or beam scattering, imprint lithography can achieve resolutions beyond the limitations set by diffraction. Its resolution depends mainly on the minimum template feature size that can be fabricated, oftentimes with electron beam lithography. Among its many attractive attributes are high resolution, low cost of ownership, and its ability to pattern large-area structures in both planar and roll-to-roll formats, to mention but a few. One significant advantage of imprint lithography over standard photolithography is its ability to pattern three-dimensional (3D) topographies in a single step, thus reducing the cost of fabricating such a device.<sup>1</sup> Such topographies are critical for connecting different layers on an

---

<sup>1</sup>S. Y. Chou, P. R. Krauss, and P. J. Renstrom, “Imprint of sub 25 nm vias and trenches in polymers,” *Appl. Phys. Lett.* **67**, 3114–3116 (1995).

# Chapter 11

## Lithographic Electrochemistry

“Much have I traveled in the realms of gold  
And many goodly states and kingdoms seen.”

John Keats, *On First Looking in Chapman's Homer*

### 11.1 Introduction

Some lithographic operations and processes are based on electrochemical phenomena. Two notable examples include (1) corrosion of metallic chrome (Cr) and molybdenum silicon (MoSi) absorber structures in optical masks and (2) electrochemical imprint lithography. Both phenomena are based on electrochemical anodic oxidation. We explore in this chapter the electrochemical basis of these two phenomena.

#### 11.1.1 Corrosion in lithography

Like most metals in everyday use, metals used in lithography tend to revert to their thermodynamically stable state, which is usually an oxide; as examples, chromium oxide is the basis of the scale or crud on corroded chrome mask absorbers in optical lithography, and silicon dioxide is the basis of anodically oxidized patterned structures transferred to silicon substrates patterned with an electrochemical imprint mask coated with noble metals such as platinum and gold. Note that any oxidation is, strictly speaking, electrochemical in nature since it is a chemical reaction involving the transfer of electrons.

Although the formation of chromium oxide on optical lithographic masks and silicon dioxide on patterned silicon substrates is based on electrochemical anodic oxidation, the formation of each differs from the other in its essential aspects. The formation of chromium oxide crud on optical lithographic masks is an unintended process-induced consequence of a specific lithographic unit operation, namely, extended irradiation of chrome-on-glass masks in an exposure chamber with 6.4-eV photons and with an appreciable amount of residual moisture that can settle on the surface of the masks, which forms an

# Chapter 12

## Lithographic Colloidal Chemistry

“Here the boundaries meet and all contradictions exist side by side.”  
Fyodor Dostoevsky, *The Brothers Karamazov*

### 12.1 Introduction

We encounter many types of colloidal<sup>1</sup> systems in lithography. These systems involve dispersion of one finely divided or microscopic phase (typically solid particles) in another (typically a liquid).<sup>2</sup> Examples of colloidal dispersions in lithography are shown in Table 12.1. These lithographic resist colloidal solutions must be distinguished from molecular mixtures or true solutions that are encountered in lithography, such as optical lithographic photoresist formulations that are formed from the dissolution of resist polymeric resins and additives in appropriate solvents, or from the dissolution of exposed positive-tone photoresists in 0.24 N tetramethyl ammonium hydroxide aqueous developer, or from the negative-tone development of unexposed photoresists in organic solvents such as n-butyl acetate.

---

<sup>1</sup>The term *colloid* is derived from the Greek word *kola* for glue. It was originally used to refer to gelatinous polymeric colloids, which Thomas Graham identified in 1860 in his experiments on osmosis and diffusion. Today, a colloid refers to a particle in the size range of 50 Å to 50 μm. The theories that explain the characteristics of colloids, including their stability and related phenomena, are sufficiently treated within the general topics of interfacial and electrostatic phenomena in classical texts on colloid chemistry [see, for example, J. T. Davies and E. K. Rideal, *Interfacial Phenomena*, Academic Press, New York (1961)] as well as in applied texts [such as R. M. Pashley and M. E. Karaman, *Applied Colloid and Surface Chemistry*, John Wiley & Sons, Ltd., Chichester (2004)]. We adapt the formalisms of these theories to the specific cases of the colloids used in technological applications in lithographic inks and resists. We adopt the notation and aspects of the derivations used by Pashley and Karaman in their text.

<sup>2</sup>This dispersion of one finely divided phase in another is quite different from molecular mixtures.

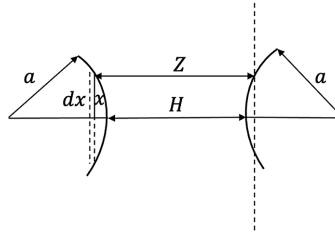


**Figure 12.10** Diagram illustrating the Derjaguin approximation for the interaction between two spherical lithographic colloidal particles.

$$V_s \approx 2\pi \int_{Z=H}^{Z=\infty} V_F x dx. \quad (12.57)$$

Rearranging Eq. (12.57), we obtain

$$V_s \approx \pi a \int_{Z=H}^{Z=\infty} V_F dZ. \quad (12.58)$$

Substituting Eq. (12.56) into Eq. (12.58), we obtain the corresponding electrostatic interaction energy between the two spheres:

$$V_s \approx 2\pi a \epsilon_0 D \psi_0^2 \exp(-\kappa H), \quad (12.59)$$

where  $H$  is the distance between the spheres. Equation (12.59) indicates that the interaction energy decays exponentially and is strongly dependent on both the surface electrostatic potential and the electrolyte concentration.

### 12.2.2 The DLVO theory of colloidal stability

The DLVO theory (named after Derjaguin, Landau, Verwey, and Overbeek) explains the tendency of colloids to agglomerate or remain stable (or dispersed). It uses the balance between two opposing forces—electrostatic repulsion and van der Waals attraction—to explain the stability of colloidal systems. We discussed repulsive electrostatic interaction in the previous section. The electrostatic interaction between two interacting spherical particles is given by Eq. (12.59). Van der Waals attraction, on the other hand, is the result of forces between individual molecules in each colloid. Its effect is additive and involves the total interaction of every molecule in one particle with that in the other particle. The van der Waals attraction between two interacting spherical colloids (Fig. 12.11) is given by

$$V_{123}(D) = -\frac{aA_{121}}{12H}, \quad (12.60)$$





**Uzodinma Okoroanyanwu**, a research associate professor in the department of polymer science and engineering of University of Massachusetts at Amherst, conducts research aimed at developing materials and devices used in electrochemical energy storage; chemical sensing; printed, flexible, flexible/hybrid and wearable electronics; and electromagnetic interference shielding. He is an SPIE Fellow and an associate editor of the *Journal of Micro/Nanopatterning, Materials, and Metrology*. He is also the founder of Enx Labs, a company that translates his research results into devices and instruments that help to improve the human condition and sustain the environment. He worked previously at Advanced Micro Devices, where he spent 12 years conducting research on advanced lithography and organic polymer memories, and at GLOBAL-FOUNDRIES, where he spent 4 years conducting research on advanced lithography. He is the author of several books, including *Chemistry and Lithography, 2nd edition, Vol. 1: The Chemical History of Lithography* (SPIE Press, 2020); *Molecular Theory of Lithography* (SPIE Press, 2015); and *Chemistry and Lithography* (SPIE Press & John Wiley & Sons, 2010). A holder of 37 U.S patents, he was educated at The University of Texas at Austin, where he earned the following degrees: Ph.D. physical chemistry (1997), M.S. chemical engineering (1995), M.A. physical chemistry (1994), B.S. chemistry and chemical engineering (1991).